A study of coke formed by heavy oil volatilization/decomposition on Y-zeolite

Ye Shui Zhang, Rhodri E. Owen, Paul R. Shearing, William C. Maskell, Dan J. L. Brett*, George Manos*

Electrochemical Innovation Lab (EIL), Department of Chemical Engineering, University College London, Torrington Place, London, WC1E 7JE

(*Corresponding authors: d.brett@ucl.ac.uk, g.manos@ucl.ac.uk)

Abstract

Coke related catalyst deactivation is still attractive for many researchers as the complexity of carbon precursor. Y-zeolite is one of the most popular catalyst used in petrochemical industry, which is also progressively degrading by coking. In this piece of work, the effects of volatilization/decomposition temperature and sample-to-catalyst ratio on the coke formed from heavy oil volatilization/decomposition in the presence of Y-zeolite catalyst have been investigated. Temperature plays a significant role in determining the nature of the carbon formed, with higher temperatures favouring a higher graphitic-to-amorphous carbon ratio. Higher sample-to-catalyst ratios lead to higher amounts of coke, but does not affect the graphitic-to-amorphous carbon ratio as the same volatilization/decomposition temperature.

Keywords: Volatilization/decomposition; Coking; Heavy oil**;** Y-Zeolite

1 Introduction

The petroleum refining industry continues to grow in line with the world's population and the corresponding increase in demand for fuels. The total oil demand is expected to reach 123 million barrels per day by 2025, according to the United States Energy Information Administration (EIA), with the production of petroleum expected at only at 61 million barrels per day, as reported by Organization of Petroleum Exporting Countries (OPEC) [1,2]. Consequently, the upgrading of petroleum residues will represent an important source of oil-based products. Petroleum vacuum residue and heavy oil are abundant sources of high-value transportation fuels after upgrading. Heavy oil usually requires thermal stimulation to be recovered from the reservoir. Heavy oil, or heavy residue fractions, are black in colour, very dense and extremely viscous, with API gravity between 10-20°. The atmospheric residue is the heavy fraction collected at the bottom of the distillation tower with an average boiling point above 343 °C, while vacuum residue is collected from the vacuum distillation tower with a boiling point above 550 °C [1].

Since 1998, approximately 617.5 million metric tons of petroleum residues have been upgraded by different processes, such as thermal, de-asphaltene, hydroprocessing and residue fluidised catalytic cracking [3]. The crude oil upgrading process can be classified as carbon rejection or thermal process, including visbreaking, steam cracking, residue fluid catalytic cracking and coking. Thermal and solvent de-asphalting are non-catalytic process; Hydroprocessing and residue fluidised catalytic cracking are catalytic processes [4].

A great deal of cracking performed industrially relies on the use of a catalyst. The catalyst properties are very important for catalytic cracking of heavy oil. Since heavy oil or vacuum residue are mixtures of high molecular weight compounds containing various impurities, which is very difficult to crack, so the acidic and porous catalysts are required for their catalytic cracking process [1,5]. Zeolite-based materials have been widely applied as cracking catalysts in the refining and petrochemical industry due to their activity, porous structure and high surface area. Zeolites are crystalline alumina-silicates made of a tetrahedron of four oxygen anions surrounding a silicon or aluminium ion as a primary building block. The structure of a zeolite is formed by the arranged combination of silica and alumina tetrahedra. Depending on the way they are arranged in the zeolitic framework, numerous different structures can be formed with different pore sizes. Y-zeolite, with faujasite structure, is one of the most widely applied types of zeolite in the catalytic cracking petroleum industry [6,7]. Zeolites have also been applied in bio-oil upgrading processes [8].

Deactivation of catalysts caused by coke formation is a major challenge and continues to receive significant attention [8-14]. For example, Wang et al. [9] used a novel thermogravimetric method to classify coke precursors on USY-zeolite into “small” and “large” categories. Chen et al. [10] used in-situ thermogravimetric analysis to investigate the multiple roles of coke precursors on USY-zeolite catalyst during the catalytic cracking of hexane. Ibarra et al. [11] reported the dual pathways for coke deactivation in the catalytic cracking of bio-oil and vacuum gas oil in fluid catalytic cracking condition. These, and other studies indicate that coke formation is correlated with reaction temperature and catalyst properties [15,16]. The deactivating effect of coke formation on zeolites is well known. Li et al. [12] investigated coke formation during bio-oil hydro-deoxygenation in the presence of Ni/HZSM-5 and Ni-Cu/HZSM-5 catalysts. Bartholomew [14] summarized the six mechanisms of catalyst deactivation: poisoning, fouling, thermal degradation, vapor compound formation, vapor-solid and or solid-solid reactions, and attrition/crushing, which are caused by chemical, mechanical and thermal reasons. The formation of carbon blocks the pores of the catalyst, and damages the catalyst structure. For example, Choi et al. [8] show how ZSM-5 zeolite pores are blocked by coke formation in the bio-oil catalytic cracking process and dramatically reduce reaction efficiency. Thus far, little research concerned with coke formed on Y-zeolite during volatilization/decomposition of heavy oil has been conducted. As temperature is one of the most influential parameters on coke formation, so this work focuses on this parameter as well as the effect of feedstock-to-catalyst ratio. This piece of work is mainly concentrate to fundamental characterization of coke formed via heavy oil volatilization/decomposition, to understand how the decomposition temperature and feedstock-to-catalyst ratio would influence the coke formation on Y-zeolite.

2 Materials and Methods

2.1 Materials

UN1267 petroleum heavy oil (Roemex^{TM}) was used for all investigations; this is solid at room temperature and black/dark brown in colour with H/C ratio at 0.16. The elemental analysis for heavy oil was obtained from SOCOTEC, UK, that the sample contains 85.87% of carbon, 13.84% of hydrogen, 0.23 % of sulphur and 0.14% of nitrogen. The heavy oil sample contains 47.78 % of saturates, 23.78 % of aromatics, 17.79 % of resins and 10.65 % of asphaltenes that was analysed by Jones Environmental, UK. The colloids asphaltene fractions in heavy oil contain nitrogen, oxygen, sulphur, vanadium and nickel compounds which is one of the reason why heavy oil in poor quality [1]. Also, the catalyst deactivation in hydroprocessing of heavy oil mainly due to the accumulation of metals and coke occupy the pores of catalyst. The deactivation may not re-generable, especially for the metal deposition that vanadium is on the surface of catalyst and the nickel distributed inside of the porous structure of the catalyst [17].

Y-zeolite with Si/Al ratio of 2.5 was provided by Grace Gmbh. Scanning electron microscopy (SEM) showed that the catalyst particles are relatively homogeneous in terms of shape and size with an average particle size of ca.1 µm. The total surface area of the Y-zeolite is 590 ± 23.5 $m^2\,g^{-1}$, with a micropore surface area of 532.4 $m^2\,g^{-1}$ and micropore volume of 0.26 $cm^3\,g^{-1}$.

The American Petroleum Institute (API) gravity of the heavy oil sample used for this work is 29.9, calculated by the following formulas [18]:

$$Specific\ Gravity\ (SG)Oil = \frac{\rho_{oil}}{\rho_{H_2O}} \tag{1}$$

$$API\ Gravity = \frac{141.5}{SG} - 131.5 \tag{2}$$

2.2 Methods

Figure 1 shows a schematic diagram of the experimental setup used for heavy oil volatilization/decomposition experiments in the presence of Y-zeolite catalyst. With this rig we studied the coke formation on Y-zeolite from volatilization/decomposition of heavy oil. A long ceramic sample holder containing both zeolite and heavy oil samples was placed inside a quartz tube reactor (inner diameter of 6.5 cm and 85 cm in length) that was heated externally by a tubular furnace. The heavy oil sample was placed in one end of the holder while the zeolite was at the other end downstream, so the volatiles from heavy oil were flowing toward zeolite. The temperature ramp rate was kept constant at 10 $^{o}C\ min^{-1}$. Nitrogen was used as the purge gas with a continuous flow at 200 $mL\ min^{-1}$. The experimental setup is aiming to grow carbon from heavy oil volatilization/decomposition products, which is an emulation for the coke formed in volatilization/decomposition process.

To investigate the effect of temperature, the sample-to-catalyst ratio was kept constant at 2:1 (1 g of heavy oil to 0.5 g of Y-zeolite) and the effect of different cracking temperatures explored (400, 500, 600, 700, 800 ^{o}C). To investigate the effect of the sample-to-catalyst ratio the cracking temperature was held constant at 500 ^{o}C and the ratio varied over the range of 1:1, 2:1, 3:1, 4:1 and 5:1. The mass of Y-zeolite was kept constant at 0.5 g for each experiment. For all experiments, the system was purged with nitrogen for 30 mins prior to the test to remove air from the reactor. For each test the furnace was held at the target temperature for at least 30 mins to allow the heavy oil sample to volatilise/decompose completely. All volatiles were flushed out of the reactor to the ventilation. The Y-zeolite samples were kept in an oven, held at 130 °C, for at least 48 h before experiments to remove the moisture contents.

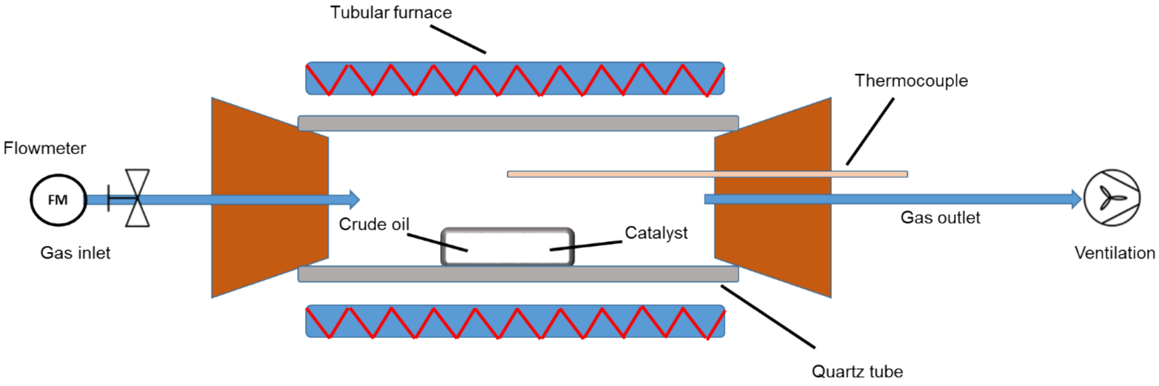

Figure 1 Schematic diagram of the setup used for heavy oil volatilization/decomposition.

2.3 Characterisation methods

The carbons deposited on the surface of the catalyst samples were analysed using temperature programmed oxidation (TPO) and thermal gravimetric analysis (TGA) (Perkin Elmer Pyris 1 TGA). Approximately 4-8 mg of each used Y-zeolite were placed in a sample crucible and heated to 900 °C with a ramp rate at 10 °C min^{-1}. For the TPO, the air flow rate was 20 mL min^{-1}, while for TGA the nitrogen flow was also 20 mL min^{-1}. The different oxidation characteristics/thermal stability of the different phases of carbon allow the proportion of these deposits to be identified. Amorphous carbon is oxidized at a lower temperature, below 600 °C, compared with the filamentous carbon, which has a higher thermal stability [19-21]. The weight loss in the TPO thermogram is due to the oxidation of deposited carbon on the Y-zeolite catalyst surface, the two peaks in the derivative thermogram at different temperatures indicate the two types of carbon oxidized at different temperatures, where the peak at lower temperature indicates the oxidation of amorphous carbon and the peak at higher temperature indicates the oxidation of graphitic carbon. The thermal stability of fresh Y-zeolite and heavy oil were also analysed by using TGA with 20 mL min^{-1} nitrogen flow. The fresh Y-zeolite was firstly heated to 120 °C with heating rate at 15 °C min^{-1}

and holding time for 30 min. Then the sample was heated to 200 ^{o}C with heating rate at 15 ^{o}C min^{-1} and holding time 30 min again. Finally, the sample was heated to 900 ^{o}C with heating rate 15 ^{o}C min and 10 min holding time. The heavy oil sample was started with heating up to 200 ^{o}C at heating rate 10 ^{o}C min^{-1}, then the sample was gradually heated to 800 ^{o}C with heating rate at 5 ^{o}C min^{-1} and holding it at 800 ^{o}C for 10 min.

A Zeiss EVO 10 scanning electron microscope (SEM) was used to characterize both the fresh Y-zeolite. A Jeol 2100 LaB_6 transmission electron microscope (TEM) was used to obtain higher magnification imaging in order to identify the types of produced carbon based on the morphology.

A Thermo Scientific^{TM} DXR Raman spectrometer with a wavelength of 532nm at Raman shifts between 100 and 3500 cm^{-1} was used to obtain Raman spectra in order to assess the degree of graphitization of the carbon formations [22-26]. Gaussian peak fitting method as one of the most common methods is used to separate two obvious peaks in Raman spectra [27,28].

3 Results and Discussion

3.1 Fresh Y-zeolite and heavy oil thermal analysis

Figure 2 shows the TGA results (a) and the corresponding differential thermal gravimetry (DTG) curve (b) of the fresh Y-zeolite. The DTG results show two obvious peaks, one at around 120 ^{o}C caused by the moisture removal and another at around 730 ^{o}C caused by the dehydroxylation of the –OH group on the surface of the Y-zeolite [29,30]. The weight loss between 120 to 200 ^{o}C is caused by the volatile moisture content and the weight loss between 200 to 800 ^{o}C could relates to the dihydroxylation of –OH group [30]. Figure 2 (a) shows that fresh Y-zeolite is stable at 400-800 ^{o}C. The TGA and DTG curves of heavy oil in Figure 3 show that the heavy oil sample starts decomposing at 300 ^{o}C and finishes before 500 ^{o}C, which explains the reason for the selection of 500 ^{o}C as the constant temperature to investigate the influence of the oil-to-catalyst ratio.

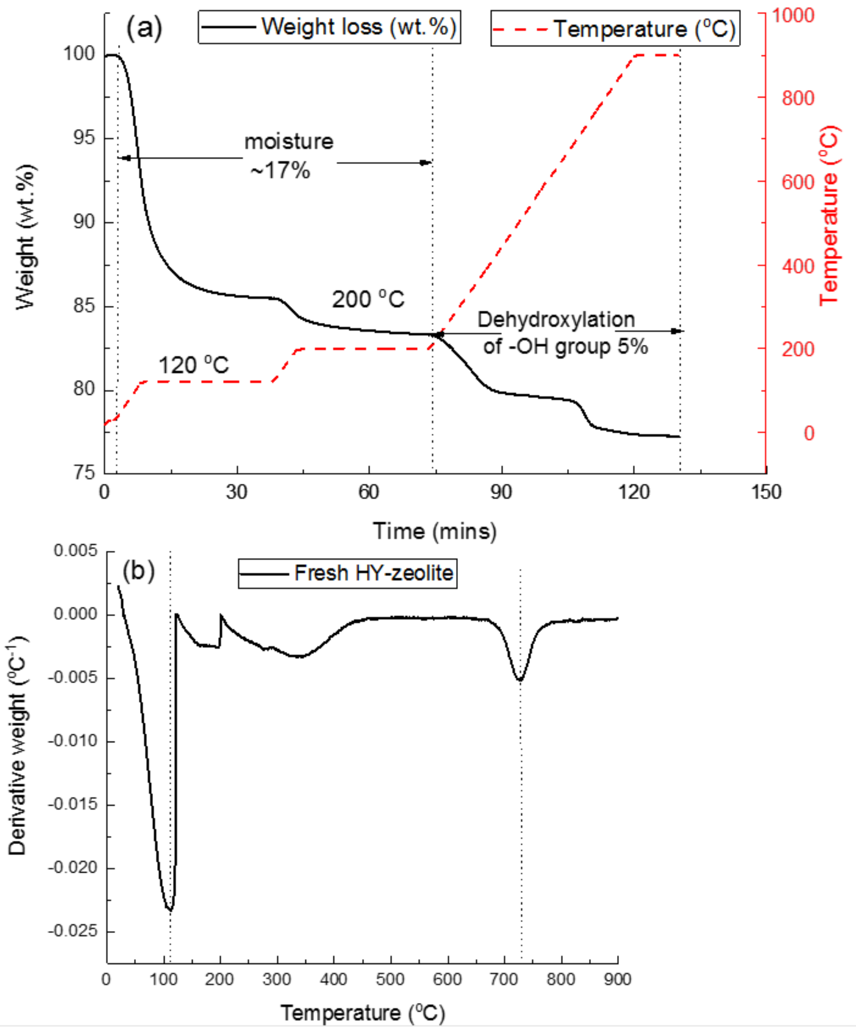

Figure 2 (a) TGA and (b) DTG of fresh Y-zeolite obtained between room temperature and 900 °C with 10 °C min^{-1} heating rate under nitrogen atmosphere.

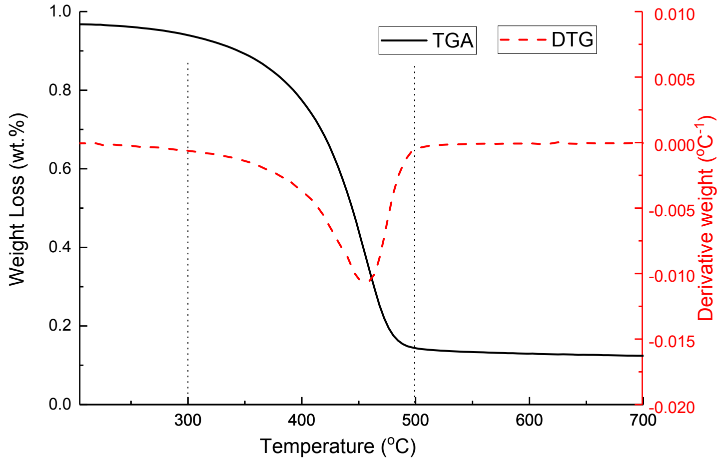

Figure 3 TGA and DTG analysis of heavy oil sample obtained between 200 °C and 700 °C at heating rate 5 °C.

3.2 Influence of temperatures on coke formation

The volatilization/decomposition of heavy oil is one of the carbon rejection reactions involved in the upgrade process. The influence of temperature on coke formation during the volatilization/decomposition of heavy oil was investigated at a sample-to-catalyst ratio of 2:1 (1 g heavy oil to 0.5 g Y-zeolite). The produced coke has been analysed by TPO, the results obtained from this study are summarised in Figure 4.

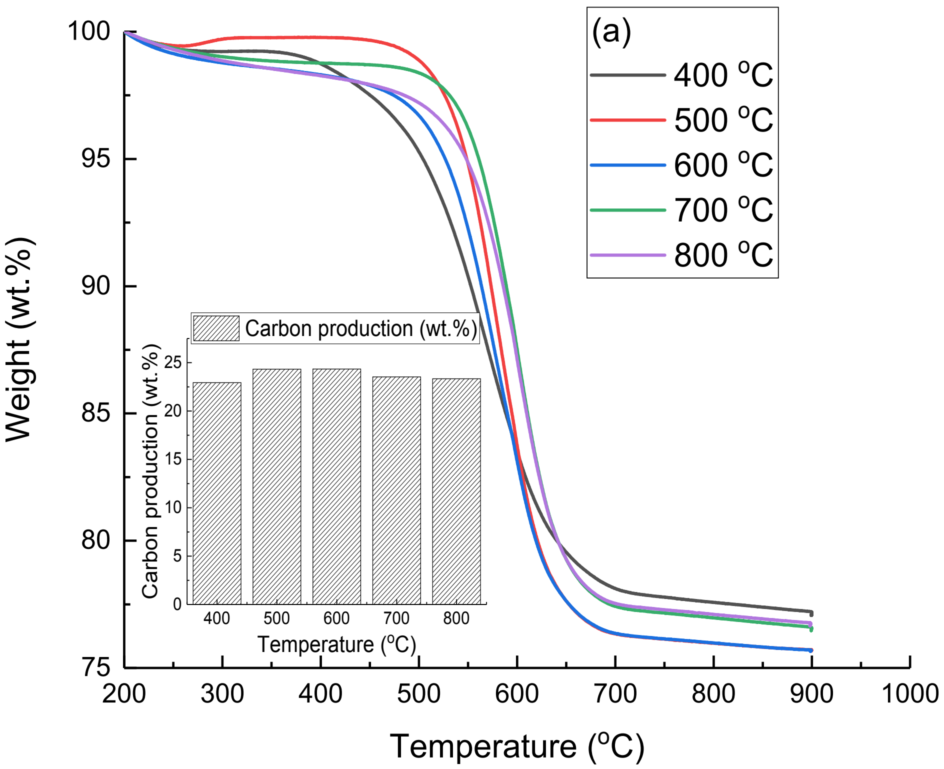

Figure 4 TPO of carbon formed from heavy oil with Y-zeolite at 400, 500, 600, 700 and 800 °C; inset carbon production derived based on TPO weight loss.

All samples showed a similar total weight loss in a range between 22.93 % - 24.34 %. The results indicate that the quantity of carbon produced from heavy oil volatilization/decomposition in the presence of Y-zeolite has no correlation to temperature. The DTG curves shown in Figure 5 (a) illustrate that carbon produced at all temperatures, except at a reaction temperature of 400 °C, all start oxidizing at 350 °C and complete their oxidation at 700 °C. The carbon produced at 400 °C had lower thermal stability with their oxidation starting at 300 °C. All carbons produced at 400, 500, 600 °C come with two overlapping oxidation peaks (peak 1 and 2) which indicate that the carbon produced from heavy oil at relatively low temperatures, below 600 ºC, includes two different types, amorphous and graphitic carbon. The carbons produced at 700 and 800 ºC exhibit a single sharp oxidization peak that indicates the carbons produced at a higher temperature, above 600 ºC, are mostly graphitic [20,31].

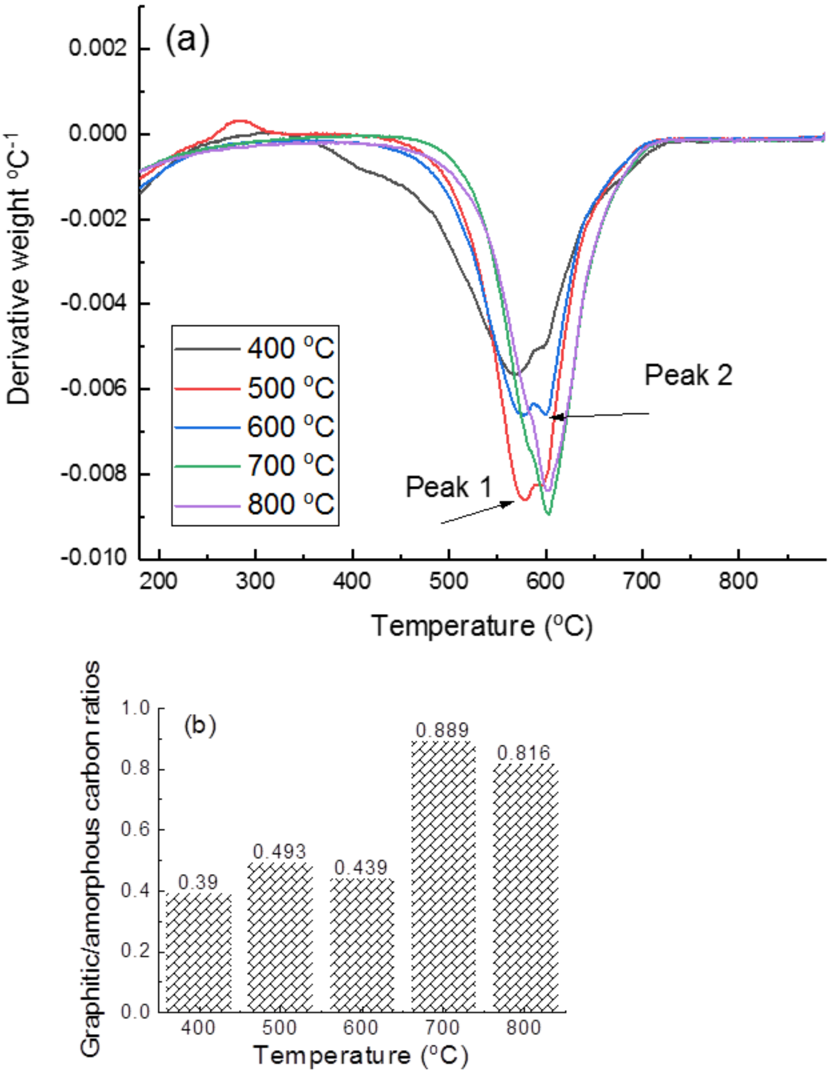

Figure 5 (a) DTG of carbon formed from heavy oil with Y-zeolite at 400, 500, 600, 700 and 800 ºC; (b) graphitic carbon/amorphous carbon ratios produced at 400, 500, 600, 700 and 800 ºC.

The ratios between graphitic carbon and amorphous carbon produced at different cracking temperatures are calculated based on the TPO and DTG results, as illustrated in Figure 5(b), where the carbon oxidized before 600 ºC is assumed amorphous carbon and the carbon oxidised after 600 ºC is assumed as graphitic carbon [31]. The results in Figure 5(b) confirm that the carbon formed at higher temperatures, at and above 700 ^{o}C, have much higher graphitic-to-amorphous carbon ratios, nearly twice more compared to temperatures below 700 ^{o}C. There are no significant differences for the graphitic-to-amorphous carbon ratios between the carbons formed at low temperature, between 400 to 600 ^{o}C, which are 0.39, 0.49 and 0.44, respectively. Similarly, the carbon formed at higher temperatures, 700 and 800 ^{o}C, show little difference in terms of the graphitic-to-amorphous carbon ratios, 0.89 and 0.82, respectively.

Carbon can be formed in the form of Ybridizations including sp^1, sp^2 (graphite-like) and sp^3 (diamond-like). The different carbon allotropes either contain pure single hybridization or as a mixture [25,32,33]. Raman spectroscopy is a common method to distinguish and classify the carbon products summarised in Figure 6. The D-band appearing at a Raman shift of 1375 cm^{-1} indicates the disordered/amorphous carbon, such as sp^3 bonding carbon or broken sp^2 bonding carbon or even sp^1 sites caused by the one-photon second-order process. The elastic and inelastic scattering are all included [25,26]. The G-band appearing at a Raman shift of 1590 cm^{-1} indicates the graphitic carbon (sp^2 carbon) caused by first-order scattering [23]. The Raman shift between 2500 and 2900 cm^{-1} appears as a broad G'-band which indicates the defects in the graphitic crystallinity of carbon produced at different temperatures and can be used to estimate the purity of carbon production as coupling the two-photon elastic scattering process. All sp^2 carbon materials have G' peaks in the Raman spectrum, which is characteristic of graphene and it is strongly dependent on the electronic and/or photon structure of graphene [23,25,34]. The lower intensity of the G' band indicates that the samples are less ordered, such as could be associated with impurities, which impedes the coupling effect of the two-photon process [23,25].

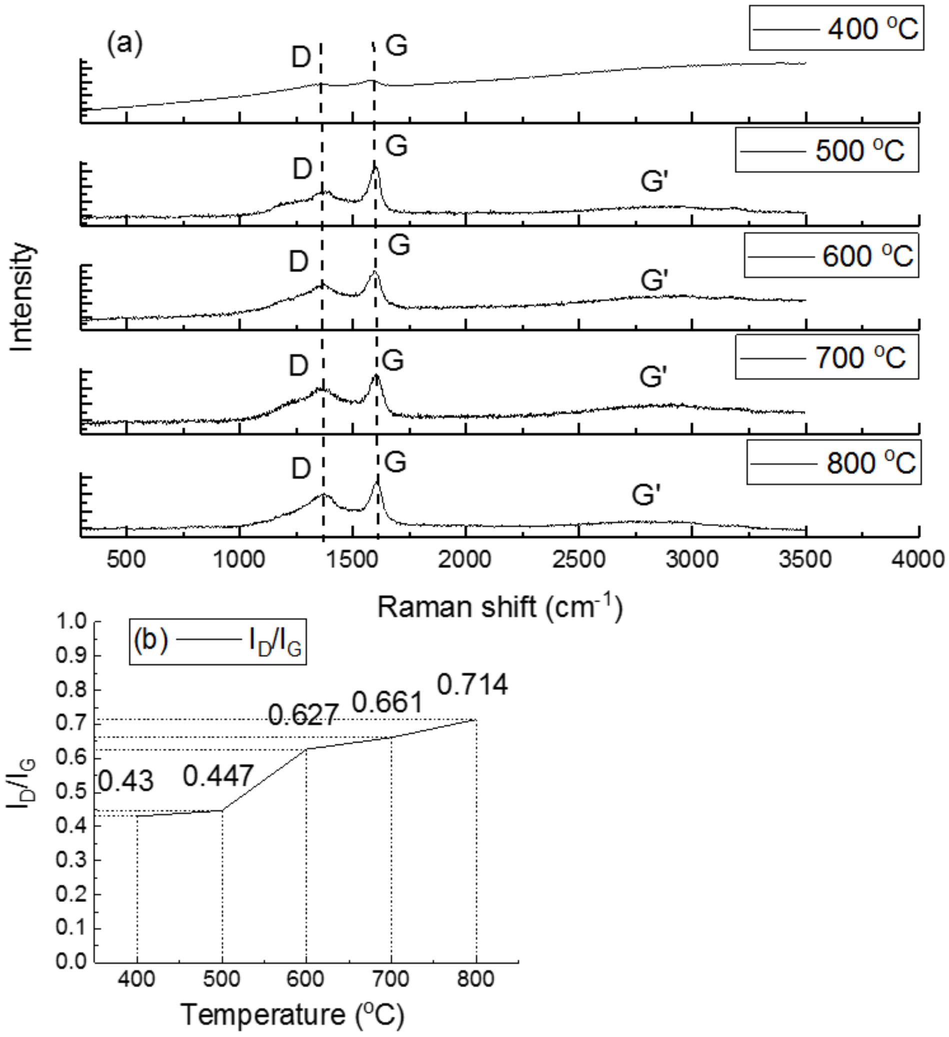

Figure 6 (a) Raman spectra with fitted peaks calculated by Gaussian method for carbon produced from heavy oil at 400, 500, 600, 700, 800 °C and Y-zeolite; (b) I_D/I_G ratios.

The baseline rise of the Raman spectrum for the carbon produced at 400 °C in Figure 6(a) is due to the resolution and the intensity of the peaks. When the resolution and the intensity are weak, the baseline will appear to slope upwards, while when the resolution and the intensity are strong, a relatively much flatter baseline can be generated in the spectra of the carbon produced at 500, 600, 700 and 800 °C, Figure 6(a). The intensity of the D-band normalized to the intensity of the G-band (I_D/I_G) can be used to determine the graphitization level of carbon [20]. Figure 6(b) shows the I_D/I_G ratios of the carbons produced from heavy oil at different temperatures. The results suggest that there is no obvious difference between the carbons produced at different temperatures. All ratios are in a quite narrow range between 0.45-0.71. Similar results have been observed in previous research that considered the graphitization level of carbon produced from difference sources such as waste tyres [20] and plastics [31]. It is difficult to draw any conclusions from these Raman results which is why the TPO was used as a supplementary method to analysis the carbon formed on the Y-zeolite at different temperatures. The TPO quite clearly shows there is a change in the carbon formed as you go to higher temperatures.

Figure 7 shows the TEM micrographs of used Y-zeolite at 400, 500, 600, 700 and 800 ^{o}C. Coke was detected in each of the reacted Y-zeolite samples at different temperatures, which is consistent with the TPO results in Figure 4. Amorphous carbon is more obvious in the used Y-zeolite reacted at temperature at 400 and 500 ^{o}C and both graphitic and amorphous carbon are observed at relative higher temperatures at 600, 700 and 800 ^{o}C. The result could be supported by previous researcher, Lee et al. [35] successfully synthesised a LaY-zeolite templated carbon prepared at high temperature. It has a similar graphitic structure as 3D graphene-like sp^2 hybridized bonds. Amorphous are observed in all of the used Y-zeolite samples, which is consistent with the TPO and Raman results in Figure 4 and Figure 6, respectively. The TPO results in Figure 4 show the coke formed on all of the used Y-zeolite samples oxidise between 350 ^{o}C and 700 ^{o}C, which indicates that the formed coke on the Y-zeolite surface is a mixture of amorphous and graphitic carbon.

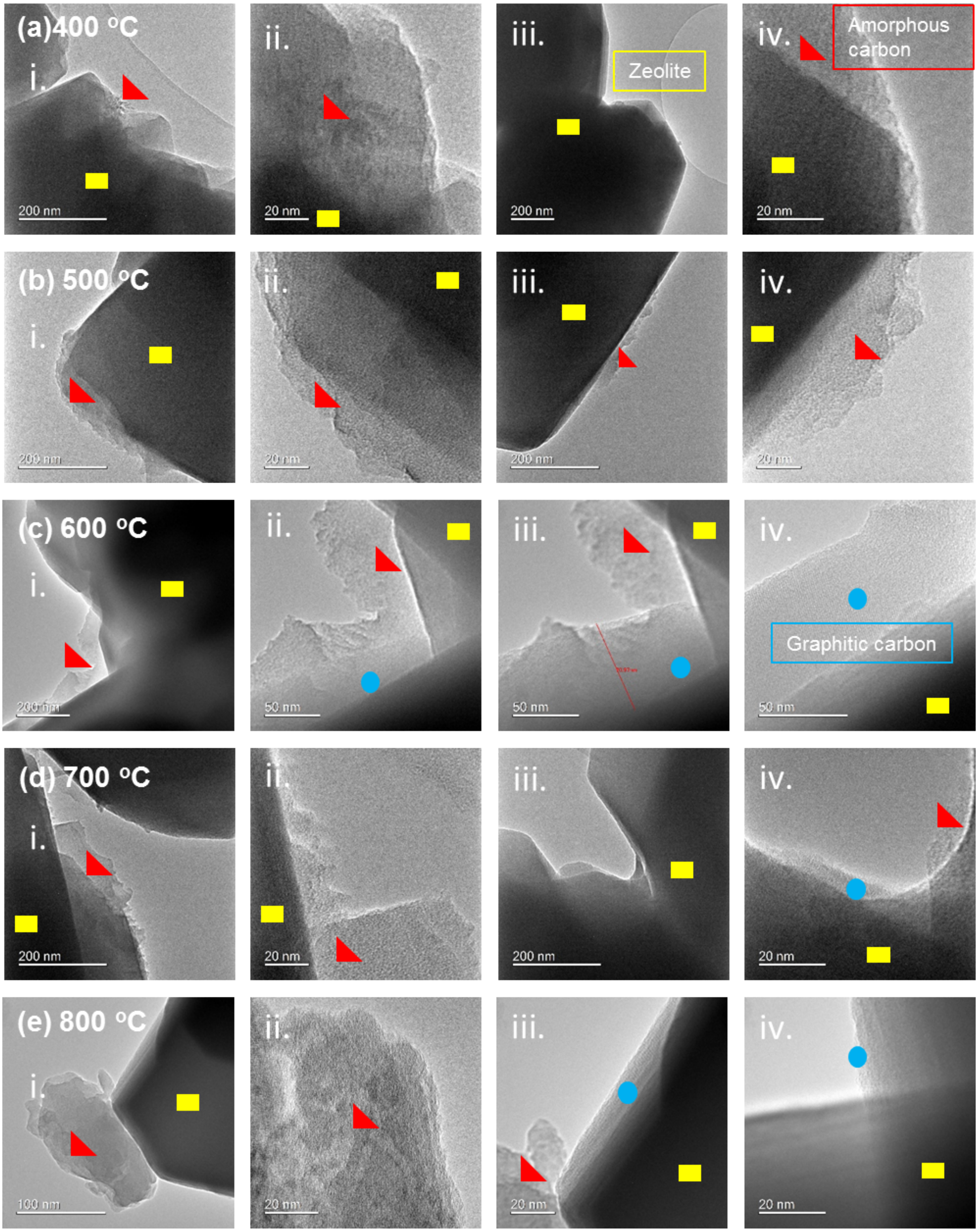
(a)400 °C
i.
200 nm
ii.
20 nm
iii.
Zeolite
200 nm
iv.
Amorphous carbon
20 nm
(b) 500 °C
i.
200 nm
ii.
20 nm
iii.
200 nm
iv.
20 nm
(c) 600 °C
i.
200 nm
ii.
50 nm
iii.
50 nm
iv.
Graphitic carbon
50 nm
(d) 700 °C
i.
200 nm
ii.
20 nm
iii.
200 nm
iv.
20 nm
(e) 800 °C
i.
100 nm
ii.
20 nm
iii.
20 nm
iv.
20 nm

(f)

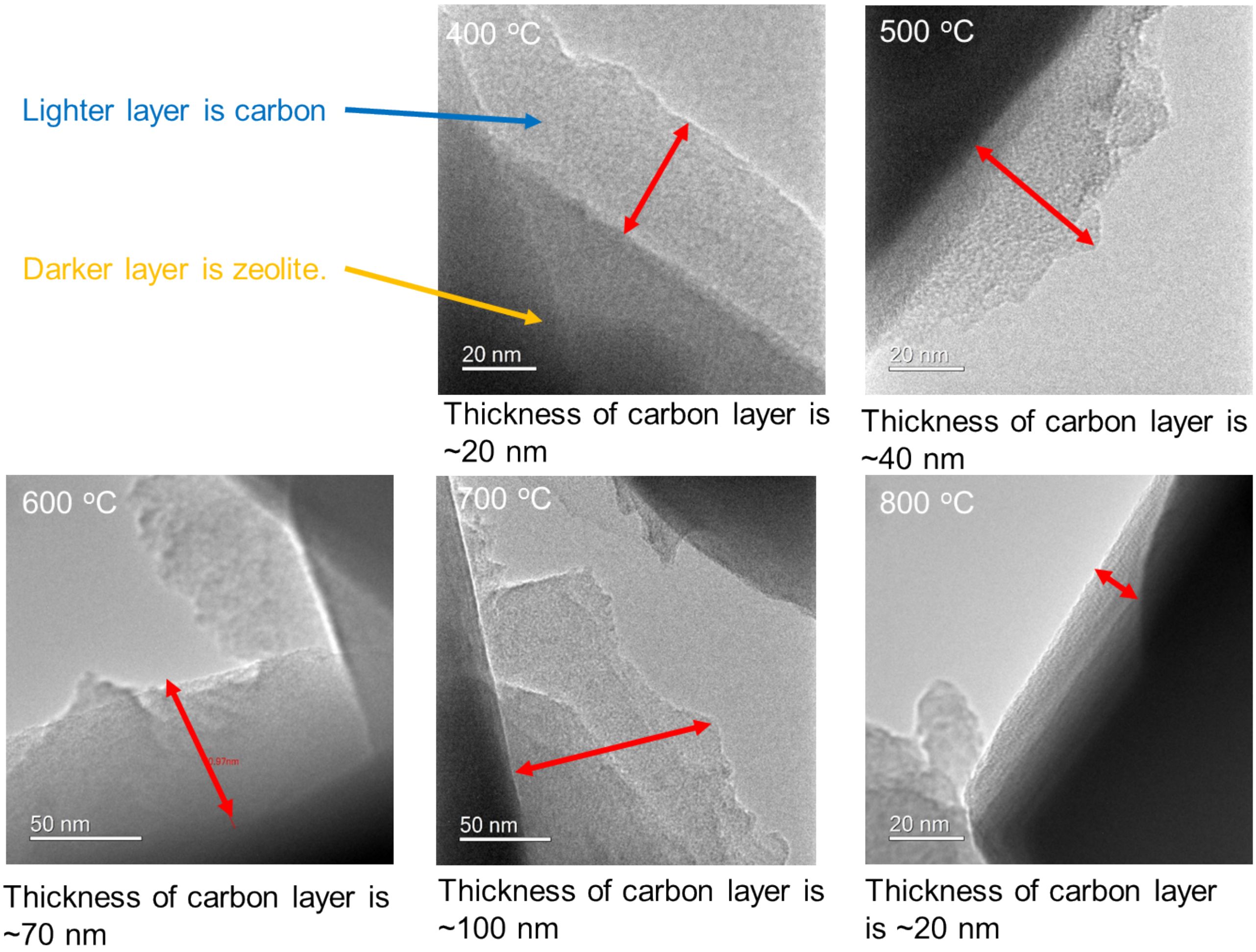

Thickness of carbon layer is ~20 nm

Thickness of carbon layer is ~40 nm

Thickness of carbon layer is ~70 nm

Thickness of carbon layer is ~100 nm

Thickness of carbon layer is ~20 nm

(g)

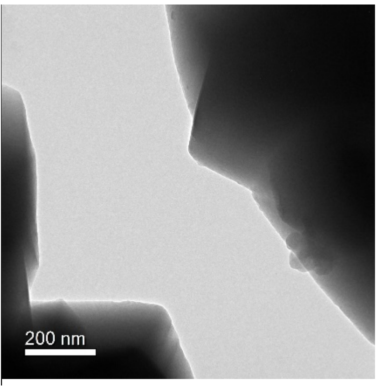

Figure 7 TEM micrographs of reacted Y-zeolite at 400, 500, 600, 700 and 800 °C. (a)-(e) carbon formed at different temperatures on Y-zeolite surface; (f) Estimation of carbon thickness on the Y-zeolite surface; (g) TEM micrograph of fresh Y-zeolite.

The Raman results in Figure 6(a) further supports this as all spectra of the coke formed on the Y-zeolite catalyst surface at different temperatures contain two peaks, one attributable to amorphous carbon the other graphitic. The thicknesses of the carbon layers on Y-zeolite catalyst surface formed at different temperatures are between 20-100 nm, as illustrated in Figure 7(f).

All of the characterisation results indicate that temperature has a strong effect on the nature of the carbon formed, especially at temperature above 600 °C. This finding is consistant with previous reports [21,36]. Acomb et al. [36] investigated the temperature effect on the production of carbon nanotubes from plastics by pyrolysis-catalysis. Previous work conducted by the authors observed that the temperature plays an important role to promote more production of highly graphitized carbon nanotubes. Zhang et al. [21] investigated the highly graphitic filamentous carbon with higher production at a higher temperature of 900 °C compared with 700 °C in the pyrolysis-catalysis of waste plastics.

3.3 Influence of sample-to-catalyst ratio on coke formation

The influence of sample-to-catalyst ratios at 1:1, 2:1, 3:1, 4:1 and 5:1 on coke formation during the volatilization/decomposition of heavy oil has been investigated at 500 °C. The amount of Y-zeolite catalyst was kept constant at 0.5 g for all of the experiments. The used Y-zeolite samples were analysed by using TPO with the results presented in Figure 8 (a). The results show in Figure 8 inset reveal that the increase of sample-to-catalyst ratio increases the quantity of formed coke, as expected, since the amount of carbon precursor increases.

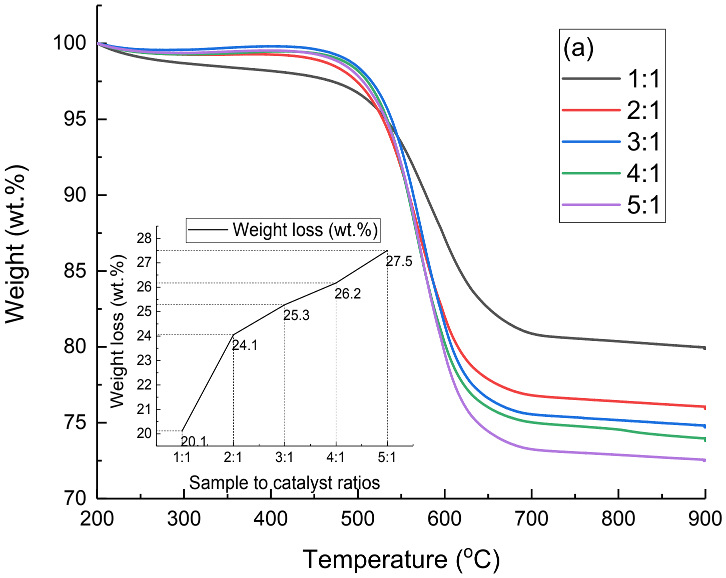

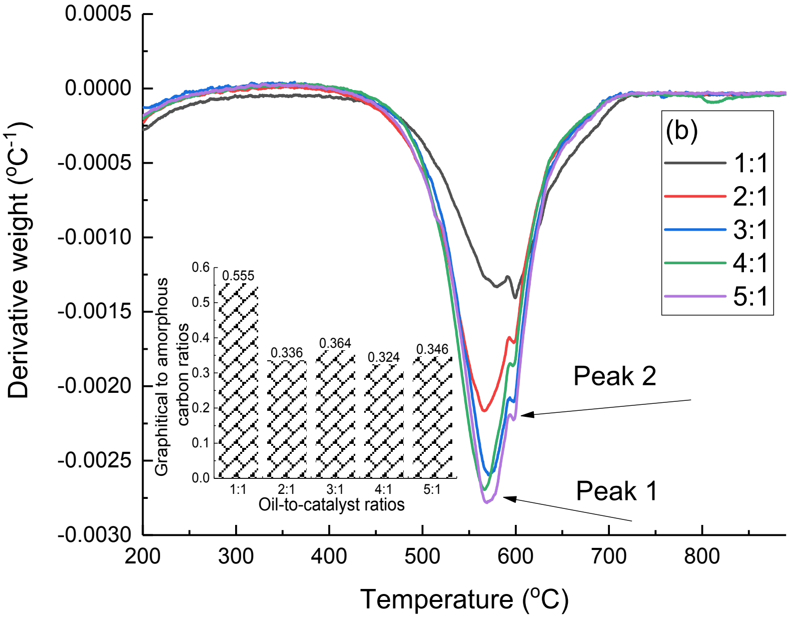

Figure 8 (a)TPO, inset figure is the derived carbon production based on TPO weight loss and (b) DTG results of carbon produced from oil at 500 °C in the presence of Y-zeolite with a sample-to-catalyst ratio of 1:1, 2:1, 3:1, 4:1 and 5:1;(b)Inset, graphitic/amorphous carbon ratios produced at oil-to-catalyst ratio at different oil-to-catalyst ratios.

Figure 8(b) presents the DTG-TPO results of the carbon formed at different sample-to-catalyst ratios. They are all similar with two overlapping oxidation peaks at around 560 (peak 1) and 600 °C (peak 2), respectively. The results indicate the degree of graphitization of the coke formed is not related to the sample-to-catalyst ratio. These results are further confirmed by the Raman analysis, as shown in Figure 9. All the coke samples formed at 500 °C with different sample-to-catalyst ratios have a D-band at 1375 cm^{-1} and G-band at 1590 cm^{-1} as shown in Figure 9 (a). The degree of graphitization of the coke formed at different sample-to-catalyst ratios are similar, with I_D/I_G ratios between 0.505 and 0.817 as shown in Figure 9 (b). The results are supported by other researchers [36]. Acomb et al. [36] found that the increment of feedstock will increase the production of carbon production, especially of highly graphitizated carbon nanotubes. Figure 8 (a)TPO, inset figure is the derived carbon production based on TPO weight loss and (b) DTG results of carbon produced from oil at 500 °C in the presence of Y-zeolite with a sample-to-catalyst ratio of 1:1, 2:1, 3:1, 4:1 and 5:1;(b)Inset, graphitic/amorphous carbon ratios produced at oil-to-catalyst ratio at different oil-to-catalyst ratios. Figure 8 (b) inset shows the quantitative ratios of graphitic/amorphous carbon are in different trend, where the 1:1 ratio gave the highest ratio at 0.555. The graphitic/amorphous ratios of carbon produced at other oil-to-catalyst ratios (2:1, 3:1, 4:1 and 5:1) are similar ~ 0.34 ± 0.023. This could relates to the deactivation of the catalyst occurs at oil-to-catalyst ratio at 1:1, the further increase amount of the oil will not lead to graphitic carbon growth but the amorphous carbon .

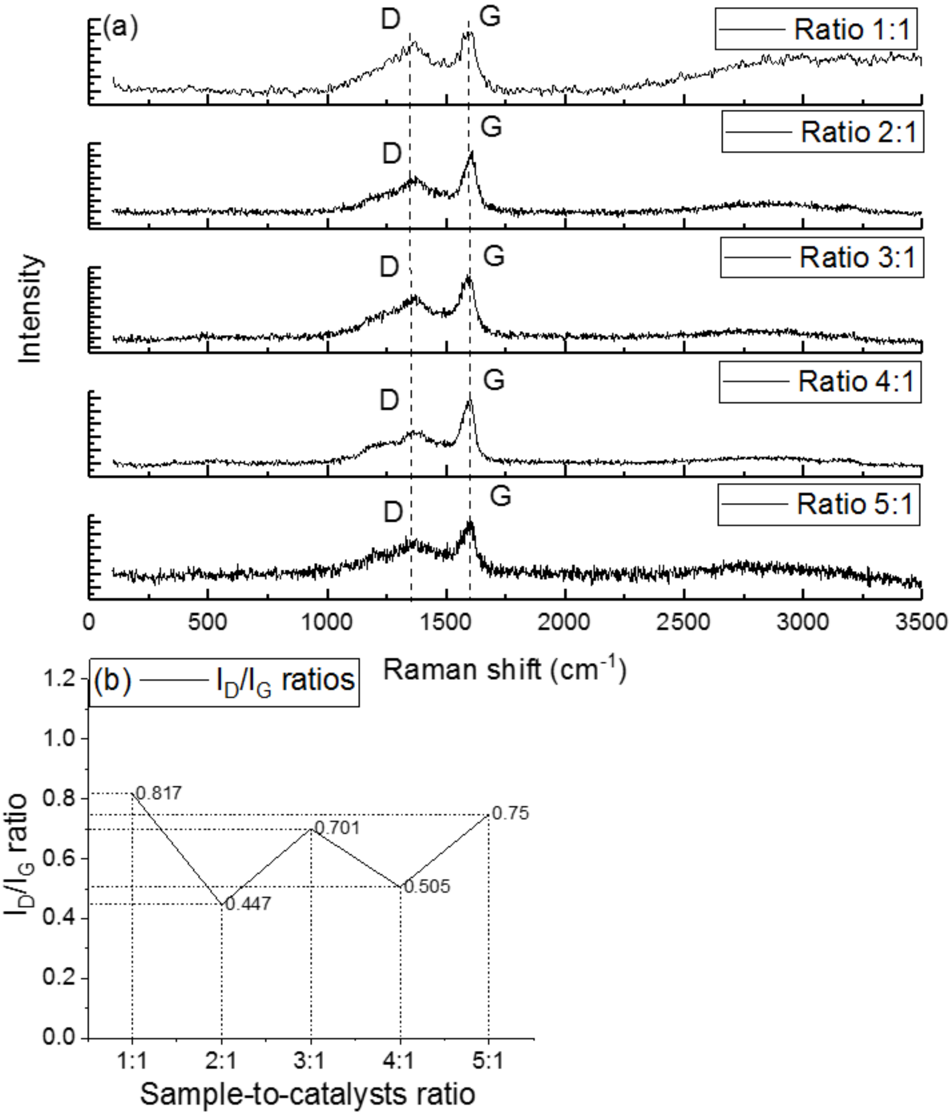

Figure 9 (a)Raman results of carbon produced from oil at 500 °C in the presence of Y- zeolite with sample-to-catalyst ratios of 1:1, 2:1, 3:1, 4:1 and 5:1; (b) I_D/I_G ratios.

4 Conclusion

Coke was found in all of the used Y-zeolite samples following volatilization/decomposition of heavy oil in a tubular reactor, regardless of reaction temperature and sample-to-catalyst ratios. However, the volatilization/decomposition temperature plays an important role on the formation of coke to deactivate the catalyst in terms of the graphitization level, but not the quantity of the carbon formed on Y-zeolite catalyst. Although the volatilization/decomposition temperature increased from 400 to 800 ^{o}C, the quantity of coke production is in a small range of 23-24% per gram of heavy oil sample. The higher temperatures of 700 and 800 ^{o}C promote more graphitic carbon production, with graphitic-to-amorphous ratios of 0.89 and 0.82, respectively. Lower temperatures, 400, 500 and 600 ^{o}C, hinder the graphitic carbon formation, which is approximately half of the graphitic carbon produced at temperatures above 600 ^{o}C. The results have been confirmed by TPO and TEM analysis. But it is difficult to analysis coke based on Raman spectra whereas TPO is an ideal technique to reveal more information about the nature of the carbon grown on Y-zeolite at different temperature in heavy oil thermal cracking process. The sample-to-catalyst ratio plays a significant role in the quantity of coke formed, rather than on the graphitic-to-amorphous ratio as the carbon source is increased but not the formation temperature. Higher sample-to-catalyst ratios form higher amounts of coke on Y-zeolite catalyst, as confirmed by TPO and Raman spectroscopy.

Acknowledgements

This work is financially supported by Qatar National Research Fund (QNRF) from National Priority Research Program (NPRP9-313-2-135).

References:

[1] R. Sahu, B.J. Song, J.S. Im, Y.-P. Jeon and C.W. Lee, A review of recent advances in catalytic hydrocracking of heavy residues, *Journal of Industrial and Engineering Chemistry*, 27, (2015) 12, https://doi.org/10.1016/j.jiec.2015.01.011.

[2] EIA, in, Energy Information Administration Office of Integrated Analysis and Forecasting U.S. Department of Energy, 2003.

[3] H. Shen, Z. Ding and R. Li, Thermal conversion - an efficient way for heavy residue processing, *Proc. 15th World Petroleum Congress*, 2, (1998) 907.

[4] J.G. Speight, *The desulfurization of heavy oils and residua*, CRC Press, 1999, 294.

[5] K. Akubo, M.A. Nahil and P.T. Williams, Aromatic fuel oils produced from the pyrolysis-catalysis of polyethylene plastic with metal-impregnated zeolite catalysts, *Journal of the Energy Institute*, 92, (2019) 195, https://doi.org/10.1016/j.joei.2017.10.009.

[6] B.C. Gates, Catalytic chemistry, (1991).

[7] A.T. Sipra, N. Gao and H. Sarwar, Municipal solid waste (MSW) pyrolysis for bio-fuel production: A review of effects of MSW components and catalysts, *Fuel Processing Technology*, 175, (2018) 131, https://doi.org/10.1016/j.fuproc.2018.02.012.

[8] Y.S. Choi, Y. Elkasabi, P.C. Tarves, C.A. Mullen and A.A. Boateng, Catalytic cracking of fast and tail gas reactive pyrolysis bio-oils over HZSM-5, *Fuel Processing Technology*, 161, (2017) 132, https://doi.org/10.1016/j.fuproc.2017.03.019.

[9] B. Wang and G. Manos, A novel thermogravimetric method for coke precursor characterisation, *Journal of Catalysis*, 250, (2007) 121, https://doi.org/10.1016/j.jcat.2007.05.018.

[10] S. Chen and G. Manos, In situ thermogravimetric study of coke formation during catalytic cracking of normal hexane and 1-hexene over ultrastable Y zeolite, *Journal of Catalysis*, 226, (2004) 343, https://doi.org/10.1016/j.jcat.2004.06.004.

[11] Á. Ibarra, A. Veloso, J. Bilbao, J.M. Arandes and P. Castaño, Dual coke deactivation pathways during the catalytic cracking of raw bio-oil and vacuum gasoil in FCC conditions, *Applied Catalysis B: Environmental*, 182, (2016) 336, https://doi.org/10.1016/j.apcatb.2015.09.044.

[12] Y. Li, C. Zhang, Y. Liu, S. Tang, G. Chen, R. Zhang and X. Tang, Coke formation on the surface of Ni/HZSM-5 and Ni-Cu/HZSM-5 catalysts during bio-oil hydrodeoxygenation, *Fuel*, 189, (2017) 23, https://doi.org/10.1016/j.fuel.2016.10.047.

[13] M. Materazzi, F. Grimaldi, P.U. Foscolo, P. Cozens, R. Taylor and C. Chapman, Analysis of syngas methanation for bio-SNG production from wastes: kinetic model development and pilot scale validation, *Fuel Processing Technology*, 167, (2017) 292, https://doi.org/10.1016/j.fuproc.2017.07.009

[14] C.H. Bartholomew, Mechanisms of catalyst deactivation, *Applied Catalysis A: General*, 212, (2001) 17, https://doi.org/10.1016/S0926-860X(00)00843-7.

[15] M. Guisnet and P. Magnoux, Organic chemistry of coke formation, *Applied Catalysis A: General*, 212, (2001) 83, https://doi.org/10.1016/S0926-860X(00)00845-0.

[16] H.S. Cerqueira, G. Caeiro, L. Costa and F. Ramôa Ribeiro, Deactivation of FCC catalysts, *Journal of Molecular Catalysis A: Chemical*, 292, (2008) 1, https://doi.org/10.1016/j.molcata.2008.06.014.

[17] M.S. Rana, J. Ancheyta, S.K. Sahoo and P. Rayo, Carbon and metal deposition during the hydroprocessing of Maya crude oil, *Catalysis Today*, 220, (2014) 97, https://doi.org/10.1016/j.cattod.2013.09.030.

[18] A. Demirbas, H. Alidrisi and M.A. Balubaid, API Gravity, Sulfur Content, and Desulfurization of Crude Oil, *Petroleum Science and Technology*, 33, (2015) 93, https://doi.org/10.1080/10916466.2014.950383.

[19] C. Wu and P.T. Williams, Investigation of coke formation on Ni-Mg-Al catalyst for hydrogen production from the catalytic steam pyrolysis-gasification of polypropylene, *Applied Catalysis B: Environmental*, 96, (2010) 198, http://dx.doi.org/10.1016/j.apcatb.2010.02.022.

[20] Y. Zhang and P.T. Williams, Carbon nanotubes and hydrogen production from the pyrolysis catalysis or catalytic-steam reforming of waste tyres, *Journal of Analytical and Applied Pyrolysis*, 122, (2016) 490, https://doi.org/10.1016/j.jaap.2016.10.015.

[21] Y. Zhang, M.A. Nahil, C. Wu and P.T. Williams, Pyrolysis–catalysis of waste plastic using a nickel–stainless-steel mesh catalyst for high-value carbon products, *Environmental technology*, 38, (2017) 1, https://doi.org/10.1080/09593330.2017.1281351.

[22] W. Fang, C. Pirez, M. Capron, S. Paul, T. Raja, P.L. Dhepe, F. Dumeignil and L. Jalowiecki-Duhamel, Ce-Ni mixed oxide as efficient catalyst for H2 production and nanofibrous carbon material from ethanol in the presence of water, *RSC Advances*, 2, (2012) 9626, https://doi.org/10.1039/c2ra21701e.

[23] M.S. Dresselhaus, G. Dresselhaus, A. Jorio, A.G. Souza Filho and R. Saito, Raman spectroscopy on isolated single wall carbon nanotubes, *Carbon*, 40, (2002) 2043, http://dx.doi.org/10.1016/S0008-6223(02)00066-0.

[24] A. Carrero, J.A. Calles and A.J. Vizcaíno, Effect of Mg and Ca addition on coke deposition over Cu–Ni/SiO2 catalysts for ethanol steam reforming, *Chemical Engineering Journal*, 163, (2010) 395, http://dx.doi.org/10.1016/j.cej.2010.07.029.

[25] R.A. DiLeo, B.J. Landi and R.P. Raffaelle, Purity assessment of multiwalled carbon nanotubes by Raman spectroscopy, *Journal of Applied Physics*, 101, (2007) 064307, doi:http://dx.doi.org/10.1063/1.2712152.

[26] A.C. Ferrari and J. Robertson, Raman spectroscopy of amorphous, nanostructured, diamond–like carbon, and nanodiamond, *Philosophical Transactions of the Royal Society of London A: Mathematical, Physical and Engineering Sciences*, 362, (2004) 2477, https://doi.org/10.1098/rsta.2004.1452.

[27] M.W. Smith, I. Dallmeyer, T.J. Johnson, C.S. Brauer, J.-S. McEwen, J.F. Espinal and M. Garcia-Perez, Structural analysis of char by Raman spectroscopy: Improving band assignments through computational calculations from first principles, *Carbon*, 100, (2016) 678, https://doi.org/10.1016/j.carbon.2016.01.031.

[28] A.C. Ferrari and J. Robertson, Interpretation of Raman spectra of disordered and amorphous carbon, *Physical review B*, 61, (2000) 14095, https://doi.org/10.1103/PhysRevB.61.14095.

[29] Z. Li, K. Xie and R.C. Slade, Studies of the interaction between CuCl and HY zeolite for preparing heterogeneous CuI catalyst, *Applied Catalysis A: General*, 209, (2001) 107, https://doi.org/10.1016/S0926-860X(00)00745-6.

[30] N.A.S. Ramli and N.A.S. Amin, Fe/HY zeolite as an effective catalyst for levulinic acid production from glucose: characterization and catalytic performance, *Applied Catalysis B: Environmental*, 163, (2015) 487, https://doi.org/10.1016/j.apcatb.2014.08.031.

[31] Y. Zhang, C. Wu, M.A. Nahil and P. Williams, High-value resource recovery products from waste tyres, *Proceedings of the Institution of Civil Engineers–Waste and Resource Management*, 169, (2016) 137, https://doi.org/10.1680/jwarm.16.00001.

[32] J. Robertson, Diamond-like amorphous carbon, *Materials Science and Engineering: R: Reports*, 37, (2002) 129, https://doi.org/10.1016/S0927-796X(02)00005-0.

[33] P.R. Somani and M. Umeno, Importance of transmission electron microscopy for carbon nanomaterials research, *Modern Research and Educational Topics in Microscopy*, 3, (2007) 634.

[34] H. Heise, R. Kuckuk, A. Ojha, A. Srivastava, V. Srivastava and B. Asthana, Characterisation of carbonaceous materials using Raman spectroscopy: a comparison of carbon nanotube filters, single- and multi- walled nanotubes, graphitised porous carbon and graphite, *Journal of Raman Spectroscopy*, 40, (2009) 344, https://doi.org/10.1002/jrs.2120.

[35] H. Lee, K. Kim, S.-H. Kang, Y. Kwon, J. Hun Kim, Y.-K. Kwon, R. Ryoo and J. Young Park, Extremely high electrical conductance of microporous 3D graphene-like zeolite-templated carbon framework, *Scientific reports*, 7, (2017), https://doi.org/10.1038/s41598-017-11602-5.

[36] J.C. Acomb, C. Wu and P.T. Williams, Effect of growth temperature and feedstock:catalyst ratio on the production of carbon nanotubes and hydrogen from the pyrolysis of waste plastics, *Journal of Analytical and Applied Pyrolysis*, 113, (2015) 231, http://dx.doi.org/10.1016/j.jaap.2015.01.012.

A study of coke formed by heavy oil volatilization/decomposition on Y-zeolite

Highlights:

Coke formed on Y-zeolite produced from heavy oil volatilization/decomposition.

Characterisations of coke formed from heavy oil.

Temperature and oil-to-catalyst ratio play different roles on the coke formation.

Proportion of graphitic and amorphous carbon identified in the coke formed.

A study of coke formed by heavy oil volatilization/decomposition on Y-zeolite

Ye Shui Zhang, Rhodri E. Owen, Paul R. Shearing, William C. Maskell, Dan J. L. Brett*,
George Manos*

Electrochemical Innovation Lab (EIL), Department of Chemical Engineering, University
College London, Torrington Place, London, WC1E 7JE

(*Corresponding authors: d.brett@ucl.ac.uk, g.manos@ucl.ac.uk)

Abstract

Coke related catalyst deactivation is still attractive for many researchers as the complexity of carbon precursor. Y-zeolite is one of the most popular catalyst used in petrochemical industry, which is also progressively degrading by coking. In this piece of work, the effects of volatilization/decomposition temperature and sample-to-catalyst ratio on the coke formed from heavy oil volatilization/decomposition in the presence of Y-zeolite catalyst have been investigated. Temperature plays a significant role in determining the nature of the carbon formed, with higher temperatures favouring a higher graphitic-to-amorphous carbon ratio. Higher sample-to-catalyst ratios lead to higher amounts of coke, but does not affect the graphitic-to-amorphous carbon ratio as the same volatilization/decomposition temperature.

Keywords: Volatilization/decomposition; Coking; Heavy oil**;** Y-Zeolite

1 Introduction

The petroleum refining industry continues to grow in line with the world's population and the corresponding increase in demand for fuels. The total oil demand is expected to reach 123 million barrels per day by 2025, according to the United States Energy Information Administration (EIA), with the production of petroleum expected at only at 61 million barrels per day, as reported by Organization of Petroleum Exporting Countries (OPEC) [1,2]. Consequently, the upgrading of petroleum residues will represent an important source of oil-based products. Petroleum vacuum residue and heavy oil are abundant sources of high-value transportation fuels after upgrading. Heavy oil usually requires thermal stimulation to be recovered from the reservoir. Heavy oil, or heavy residue fractions, are black in colour, very dense and extremely viscous, with API gravity between 10-20°. The atmospheric residue is the heavy fraction collected at the bottom of the distillation tower with an average boiling point above 343 °C, while vacuum residue is collected from the vacuum distillation tower with a boiling point above 550 °C [1].

Since 1998, approximately 617.5 million metric tons of petroleum residues have been upgraded by different processes, such as thermal, de-asphaltene, hydroprocessing and residue fluidised catalytic cracking [3]. The crude oil upgrading process can be classified as carbon rejection or thermal process, including visbreaking, steam cracking, residue fluid catalytic cracking and coking. Thermal and solvent de-asphalting are non-catalytic process; Hydroprocessing and residue fluidised catalytic cracking are catalytic processes [4].

A great deal of cracking performed industrially relies on the use of a catalyst. The catalyst properties are very important for catalytic cracking of heavy oil. Since heavy oil or vacuum residue are mixtures of high molecular weight compounds containing various impurities, which is very difficult to crack, so the acidic and porous catalysts are required for their catalytic cracking process [1,5]. Zeolite-based materials have been widely applied as cracking catalysts in the refining and petrochemical industry due to their activity, porous structure and high surface area. Zeolites are crystalline alumina-silicates made of a tetrahedron of four oxygen anions surrounding a silicon or aluminium ion as a primary building block. The structure of a zeolite is formed by the arranged combination of silica and alumina tetrahedra. Depending on the way they are arranged in the zeolitic framework, numerous different structures can be formed with different pore sizes. Y-zeolite, with faujasite structure, is one of the most widely applied types of zeolite in the catalytic cracking petroleum industry [6,7]. Zeolites have also been applied in bio-oil upgrading processes [8].

Deactivation of catalysts caused by coke formation is a major challenge and continues to receive significant attention [8-14]. For example, Wang et al. [9] used a novel thermogravimetric method to classify coke precursors on USY-zeolite into “small” and “large” categories. Chen et al. [10] used in-situ thermogravimetric analysis to investigate the multiple roles of coke precursors on USY-zeolite catalyst during the catalytic cracking of hexane. Ibarra et al. [11] reported the dual pathways for coke deactivation in the catalytic cracking of bio-oil and vacuum gas oil in fluid catalytic cracking condition. These, and other studies indicate that coke formation is correlated with reaction temperature and catalyst properties [15,16]. The deactivating effect of coke formation on zeolites is well known. Li et al. [12] investigated coke formation during bio-oil hydro-deoxygenation in the presence of Ni/HZSM-5 and Ni-Cu/HZSM-5 catalysts. Bartholomew [14] summarized the six mechanisms of catalyst deactivation: poisoning, fouling, thermal degradation, vapor compound formation, vapor-solid and or solid-solid reactions, and attrition/crushing, which are caused by chemical, mechanical and thermal reasons. The formation of carbon blocks the pores of the catalyst, and damages the catalyst structure. For example, Choi et al. [8] show how ZSM-5 zeolite pores are blocked by coke formation in the bio-oil catalytic cracking process and dramatically reduce reaction efficiency. Thus far, little research concerned with coke formed on Y-zeolite during volatilization/decomposition of heavy oil has been conducted. As temperature is one of the most influential parameters on coke formation, so this work focuses on this parameter as well as the effect of feedstock-to-catalyst ratio. This piece of work is mainly concentrate to fundamental characterization of coke formed via heavy oil volatilization/decomposition, to understand how the decomposition temperature and feedstock-to-catalyst ratio would influence the coke formation on Y-zeolite.

2 Materials and Methods

2.1 Materials

UN1267 petroleum heavy oil (Roemex^{TM}) was used for all investigations; this is solid at room temperature and black/dark brown in colour with H/C ratio at 0.16. The elemental analysis for heavy oil was obtained from SOCOTEC, UK, that the sample contains 85.87% of carbon, 13.84% of hydrogen, 0.23 % of sulphur and 0.14% of nitrogen. The heavy oil sample contains 47.78 % of saturates, 23.78 % of aromatics, 17.79 % of resins and 10.65 % of asphaltenes that was analysed by Jones Environmental, UK. The colloids asphaltene fractions in heavy oil contain nitrogen, oxygen, sulphur, vanadium and nickel compounds which is one of the reason why heavy oil in poor quality [1]. Also, the catalyst deactivation in hydroprocessing of heavy oil mainly due to the accumulation of metals and coke occupy the pores of catalyst. The deactivation may not re-generable, especially for the metal deposition that vanadium is on the surface of catalyst and the nickel distributed inside of the porous structure of the catalyst [17].

Y-zeolite with Si/Al ratio of 2.5 was provided by Grace Gmbh. Scanning electron microscopy (SEM) showed that the catalyst particles are relatively homogeneous in terms of shape and size with an average particle size of ca.1 µm. The total surface area of the Y-zeolite is 590 ± 23.5 $m^2\ g^{-1}$, with a micropore surface area of 532.4 $m^2\ g^{-1}$ and micropore volume of 0.26 $cm^3\ g^{-1}$.

The American Petroleum Institute (API) gravity of the heavy oil sample used for this work is 29.9, calculated by the following formulas [18]:

$$Specific\ Gravity\ (SG)Oil = \frac{\rho_{oil}}{\rho_{H_2O}} \qquad (1)$$

$$API\ Gravity = \frac{141.5}{SG} - 131.5 \qquad (2)$$

2.2 Methods

Figure 1 shows a schematic diagram of the experimental setup used for heavy oil volatilization/decomposition experiments in the presence of Y-zeolite catalyst. With this rig we studied the coke formation on Y-zeolite from volatilization/decomposition of heavy oil. A long ceramic sample holder containing both zeolite and heavy oil samples was placed inside a quartz tube reactor (inner diameter of 6.5 cm and 85 cm in length) that was heated externally by a tubular furnace. The heavy oil sample was placed in one end of the holder while the zeolite was at the other end downstream, so the volatiles from heavy oil were flowing toward zeolite. The temperature ramp rate was kept constant at 10 °C min^{-1}. Nitrogen was used as the purge gas with a continuous flow at 200 mL min^{-1}. The experimental setup is aiming to grow carbon from heavy oil volatilization/decomposition products, which is an emulation for the coke formed in volatilization/decomposition process.

To investigate the effect of temperature, the sample-to-catalyst ratio was kept constant at 2:1 (1 g of heavy oil to 0.5 g of Y-zeolite) and the effect of different cracking temperatures explored (400, 500, 600, 700, 800 °C). To investigate the effect of the sample-to-catalyst ratio the cracking temperature was held constant at 500 °C and the ratio varied over the range of 1:1, 2:1, 3:1, 4:1 and 5:1. The mass of Y-zeolite was kept constant at 0.5 g for each experiment. For all experiments, the system was purged with nitrogen for 30 mins prior to the test to remove air from the reactor. For each test the furnace was held at the target temperature for at least 30 mins to allow the heavy oil sample to volatilise/decompose completely. All volatiles were flushed out of the reactor to the ventilation. The Y-zeolite samples were kept in an oven, held at 130 °C, for at least 48 h before experiments to remove the moisture contents.

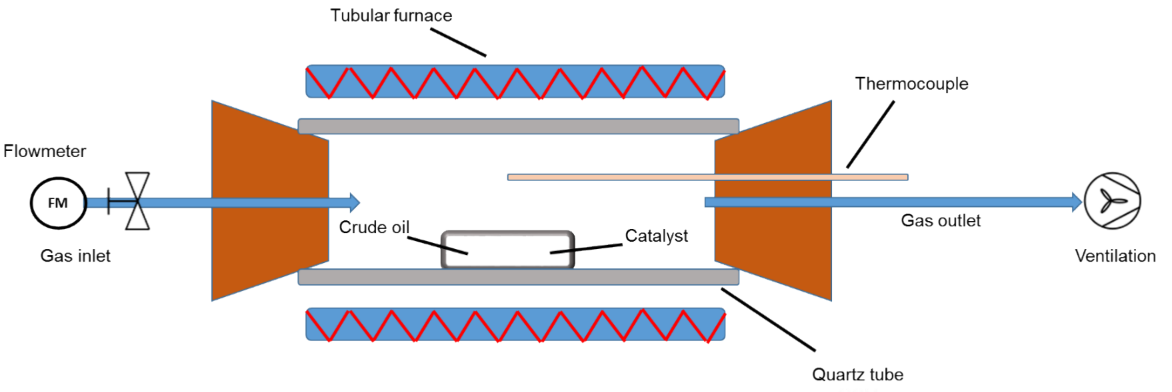

Figure 1 Schematic diagram of the setup used for heavy oil volatilization/decomposition.

2.3 Characterisation methods

The carbons deposited on the surface of the catalyst samples were analysed using temperature programmed oxidation (TPO) and thermal gravimetric analysis (TGA) (Perkin Elmer Pyris 1 TGA). Approximately 4-8 mg of each used Y-zeolite were placed in a sample crucible and heated to 900 °C with a ramp rate at 10 °C min^{-1}. For the TPO, the air flow rate was 20 mL min^{-1}, while for TGA the nitrogen flow was also 20 mL min^{-1}. The different oxidation characteristics/thermal stability of the different phases of carbon allow the proportion of these deposits to be identified. Amorphous carbon is oxidized at a lower temperature, below 600 °C, compared with the filamentous carbon, which has a higher thermal stability [19-21]. The weight loss in the TPO thermogram is due to the oxidation of deposited carbon on the Y-zeolite catalyst surface, the two peaks in the derivative thermogram at different temperatures indicate the two types of carbon oxidized at different temperatures, where the peak at lower temperature indicates the oxidation of amorphous carbon and the peak at higher temperature indicates the oxidation of graphitic carbon. The thermal stability of fresh Y-zeolite and heavy oil were also analysed by using TGA with 20 mL min^{-1} nitrogen flow. The fresh Y-zeolite was firstly heated to 120 °C with heating rate at 15 °C min^{-1}

and holding time for 30 min. Then the sample was heated to 200 °C with heating rate at 15 °C min^{-1} and holding time 30 min again. Finally, the sample was heated to 900 °C with heating rate 15 °C min and 10 min holding time. The heavy oil sample was started with heating up to 200 °C at heating rate 10 °C min^{-1}, then the sample was gradually heated to 800 °C with heating rate at 5 °C min^{-1} and holding it at 800 °C for 10 min.

A Zeiss EVO 10 scanning electron microscope (SEM) was used to characterize both the fresh Y-zeolite. A Jeol 2100 LaB_6 transmission electron microscope (TEM) was used to obtain higher magnification imaging in order to identify the types of produced carbon based on the morphology.

A Thermo Scientific^{TM} DXR Raman spectrometer with a wavelength of 532nm at Raman shifts between 100 and 3500 cm^{-1} was used to obtain Raman spectra in order to assess the degree of graphitization of the carbon formations [22-26]. Gaussian peak fitting method as one of the most common methods is used to separate two obvious peaks in Raman spectra [27,28].

3 Results and Discussion

3.1 Fresh Y-zeolite and heavy oil thermal analysis

Figure 2 shows the TGA results (a) and the corresponding differential thermal gravimetry (DTG) curve (b) of the fresh Y-zeolite. The DTG results show two obvious peaks, one at around 120 °C caused by the moisture removal and another at around 730 °C caused by the dehydroxylation of the –OH group on the surface of the Y-zeolite [29,30]. The weight loss between 120 to 200 °C is caused by the volatile moisture content and the weight loss between 200 to 800 °C could relates to the dihydroxylation of –OH group [30]. Figure 2 (a) shows that fresh Y-zeolite is stable at 400-800 °C. The TGA and DTG curves of heavy oil in Figure 3 show that the heavy oil sample starts decomposing at 300 °C and finishes before 500 °C, which explains the reason for the selection of 500 °C as the constant temperature to investigate the influence of the oil-to-catalyst ratio.

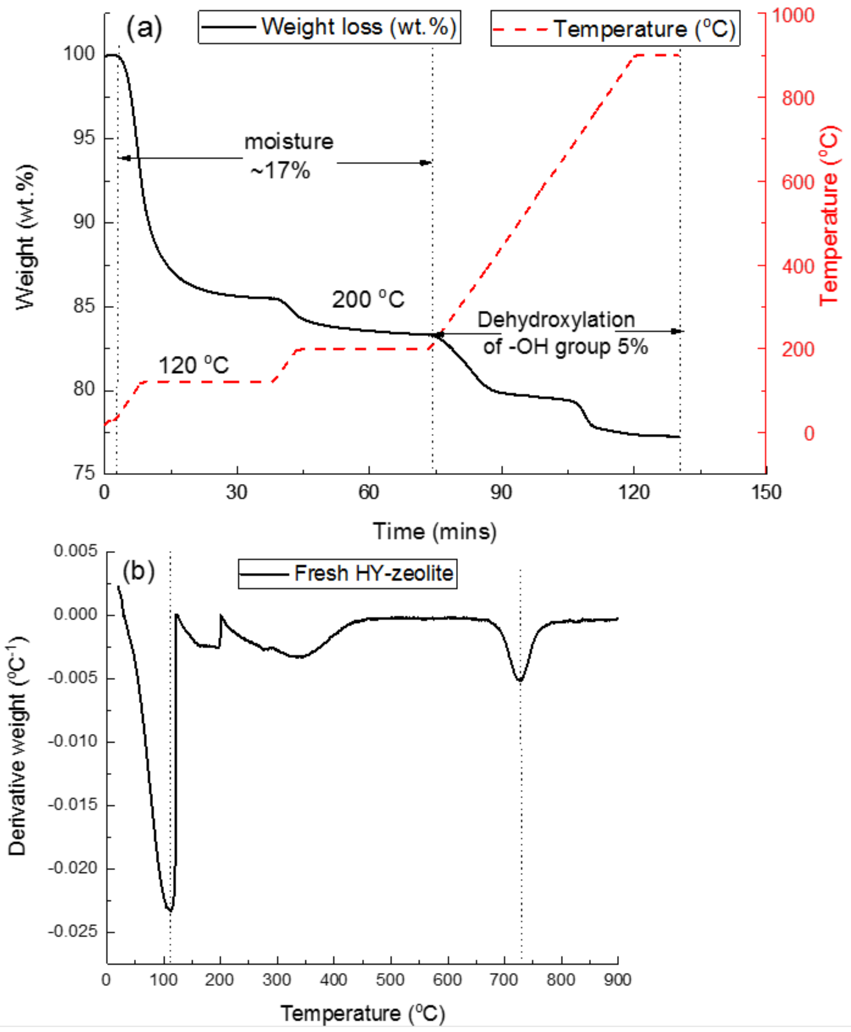

Figure 2 (a) TGA and (b) DTG of fresh Y-zeolite obtained between room temperature and 900 °C with 10 °C min^{-1} heating rate under nitrogen atmosphere.

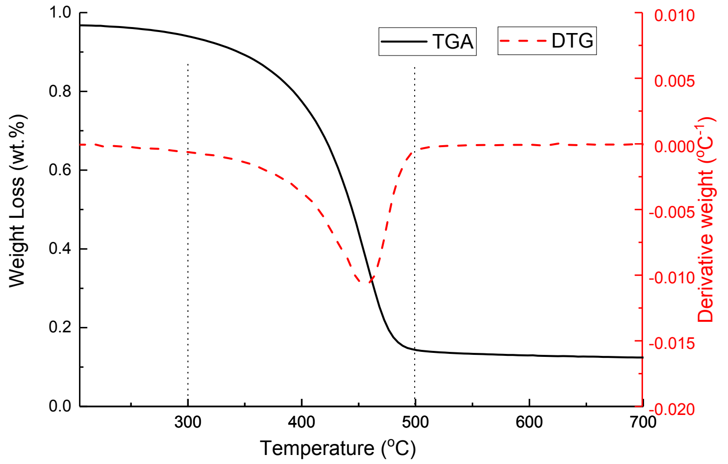

Figure 3 TGA and DTG analysis of heavy oil sample obtained between 200 °C and 700 °C at heating rate 5 °C.

3.2 Influence of temperatures on coke formation

The volatilization/decomposition of heavy oil is one of the carbon rejection reactions involved in the upgrade process. The influence of temperature on coke formation during the volatilization/decomposition of heavy oil was investigated at a sample-to-catalyst ratio of 2:1 (1 g heavy oil to 0.5 g Y-zeolite). The produced coke has been analysed by TPO, the results obtained from this study are summarised in Figure 4.

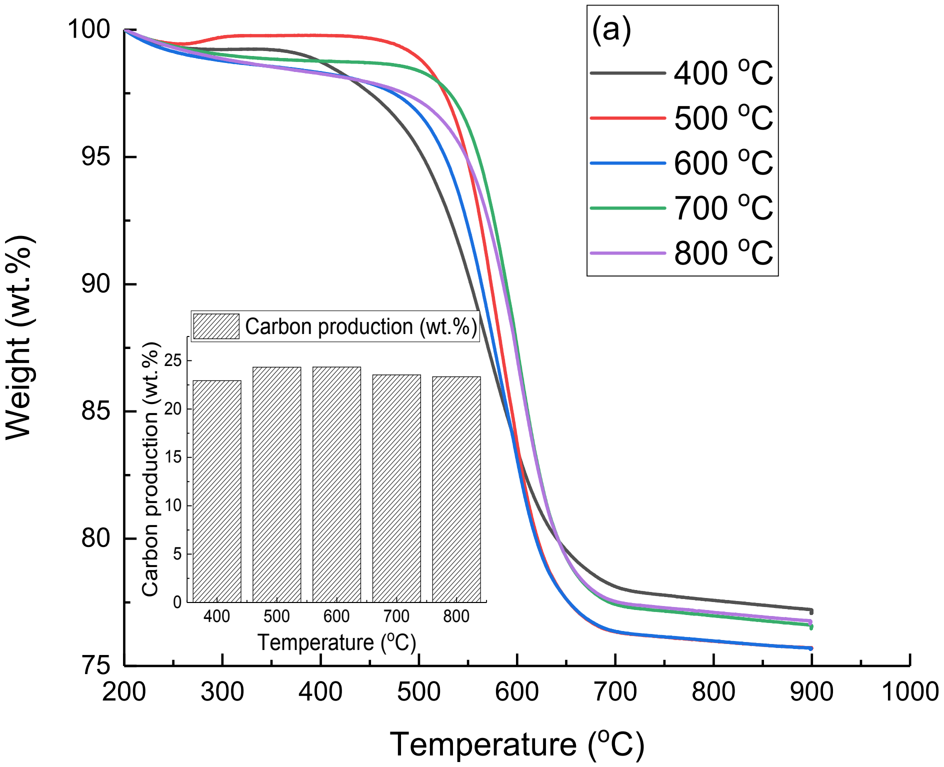

Figure 4 TPO of carbon formed from heavy oil with Y-zeolite at 400, 500, 600, 700 and 800 °C; inset carbon production derived based on TPO weight loss.

All samples showed a similar total weight loss in a range between 22.93 % - 24.34 %. The results indicate that the quantity of carbon produced from heavy oil volatilization/decomposition in the presence of Y-zeolite has no correlation to temperature. The DTG curves shown in Figure 5 (a) illustrate that carbon produced at all temperatures, except at a reaction temperature of 400 °C, all start oxidizing at 350 °C and complete their oxidation at 700 °C. The carbon produced at 400 °C had lower thermal stability with their oxidation starting at 300 °C. All carbons produced at 400, 500, 600 °C come with two overlapping oxidation peaks (peak 1 and 2) which indicate that the carbon produced from heavy oil at relatively low temperatures, below 600 °C, includes two different types, amorphous and graphitic carbon. The carbons produced at 700 and 800 °C exhibit a single sharp oxidization peak that indicates the carbons produced at a higher temperature, above 600 °C, are mostly graphitic [20,31].

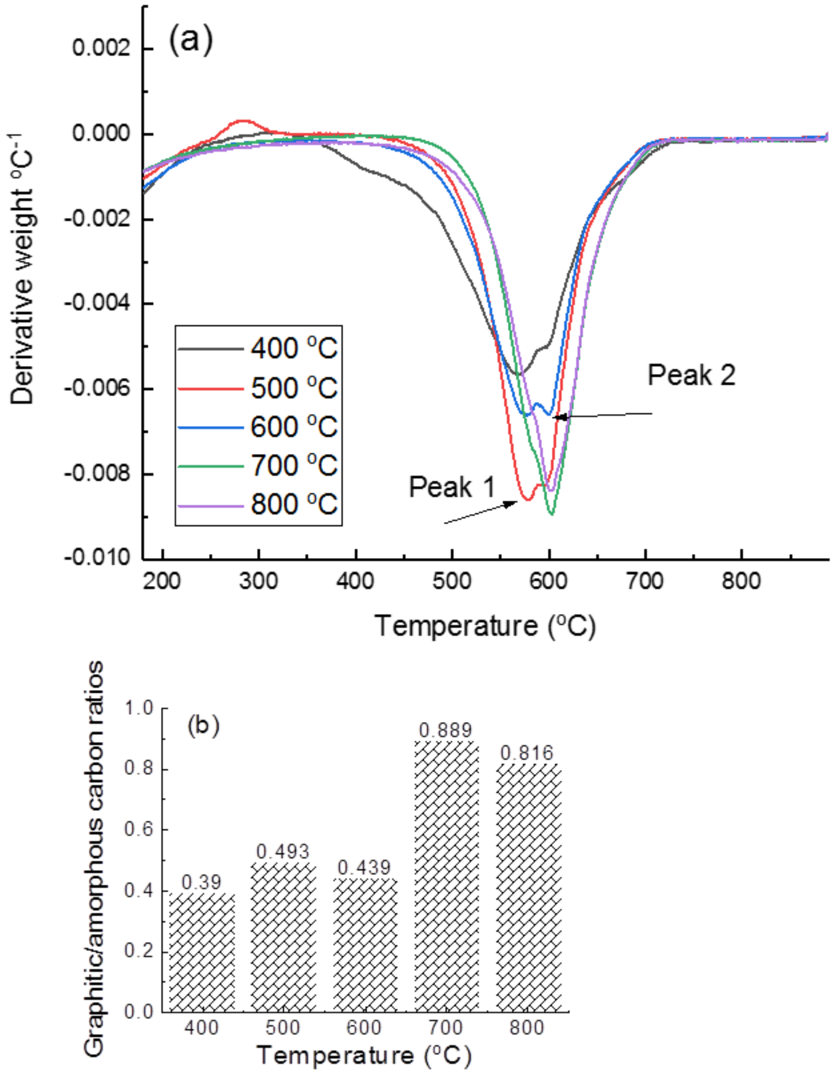

Figure 5 (a) DTG of carbon formed from heavy oil with Y-zeolite at 400, 500, 600, 700 and 800 °C; (b) graphitic carbon/amorphous carbon ratios produced at 400, 500, 600, 700 and 800 °C.

The ratios between graphitic carbon and amorphous carbon produced at different cracking temperatures are calculated based on the TPO and DTG results, as illustrated in Figure 5(b), where the carbon oxidized before 600 °C is assumed amorphous carbon and the carbon oxidised after 600 °C is assumed as graphitic carbon [31]. The results in Figure 5(b) confirm that the carbon formed at higher temperatures, at and above 700 ^{o}C, have much higher graphitic-to-amorphous carbon ratios, nearly twice more compared to temperatures below 700 ^{o}C. There are no significant differences for the graphitic-to-amorphous carbon ratios between the carbons formed at low temperature, between 400 to 600 ^{o}C, which are 0.39, 0.49 and 0.44, respectively. Similarly, the carbon formed at higher temperatures, 700 and 800 ^{o}C, show little difference in terms of the graphitic-to-amorphous carbon ratios, 0.89 and 0.82, respectively.

Carbon can be formed in the form of Ybridizations including sp^{1}, sp^{2} (graphite-like) and sp^{3} (diamond-like). The different carbon allotropes either contain pure single hybridization or as a mixture [25,32,33]. Raman spectroscopy is a common method to distinguish and classify the carbon products summarised in Figure 6. The D-band appearing at a Raman shift of 1375 cm^{-1} indicates the disordered/amorphous carbon, such as sp^{3} bonding carbon or broken sp^{2} bonding carbon or even sp^{1} sites caused by the one-photon second-order process. The elastic and inelastic scattering are all included [25,26]. The G-band appearing at a Raman shift of 1590 cm^{-1} indicates the graphitic carbon (sp^{2} carbon) caused by first-order scattering [23]. The Raman shift between 2500 and 2900 cm^{-1} appears as a broad G'-band which indicates the defects in the graphitic crystallinity of carbon produced at different temperatures and can be used to estimate the purity of carbon production as coupling the two-photon elastic scattering process. All sp^{2} carbon materials have G' peaks in the Raman spectrum, which is characteristic of graphene and it is strongly dependent on the electronic and/or photon structure of graphene [23,25,34]. The lower intensity of the G' band indicates that the samples are less ordered, such as could be associated with impurities, which impedes the coupling effect of the two-photon process [23,25].

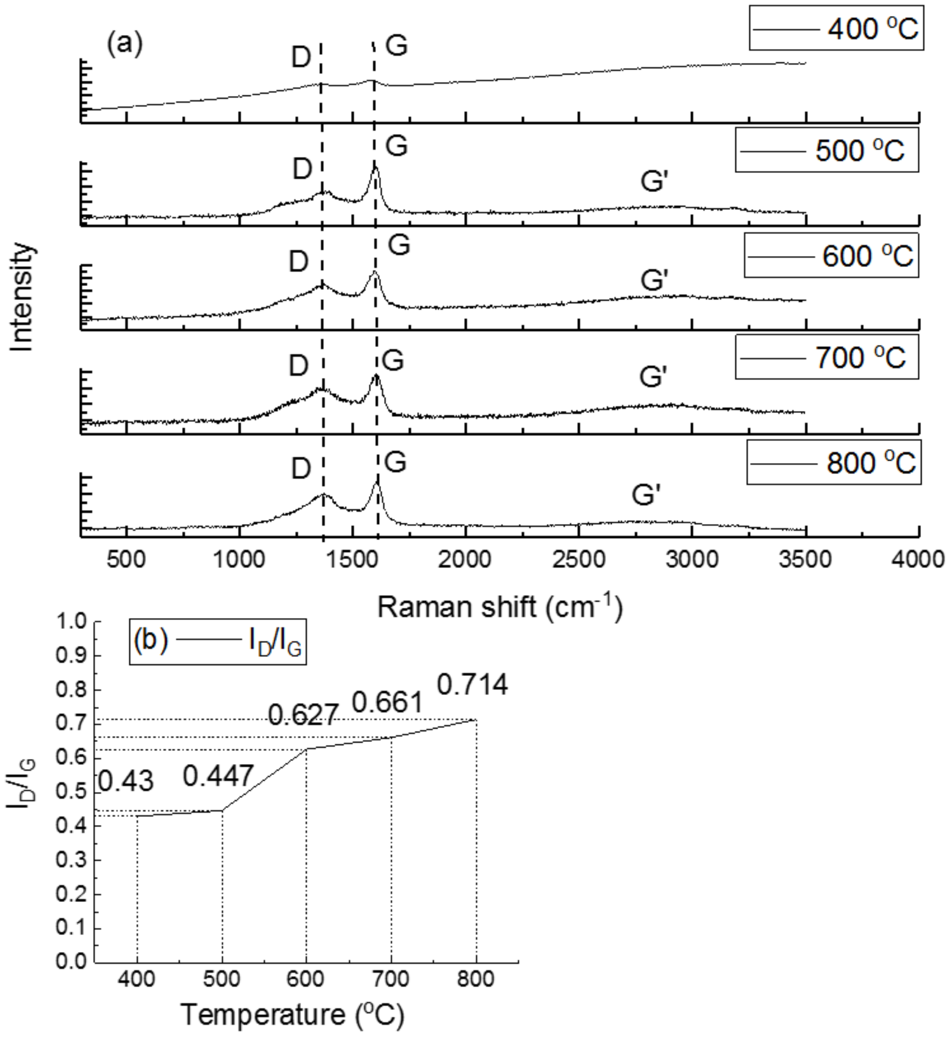

Figure 6 (a) Raman spectra with fitted peaks calculated by Gaussian method for carbon produced from heavy oil at 400, 500, 600, 700, 800 °C and Y-zeolite; (b) I_D/I_G ratios.

The baseline rise of the Raman spectrum for the carbon produced at 400 °C in Figure 6(a) is due to the resolution and the intensity of the peaks. When the resolution and the intensity are weak, the baseline will appear to slope upwards, while when the resolution and the intensity are strong, a relatively much flatter baseline can be generated in the spectra of the carbon produced at 500, 600, 700 and 800 °C, Figure 6(a). The intensity of the D-band normalized to the intensity of the G-band (I_D/I_G) can be used to determine the graphitization level of carbon [20]. Figure 6(b) shows the I_D/I_G ratios of the carbons produced from heavy oil at different temperatures. The results suggest that there is no obvious difference between the carbons produced at different temperatures. All ratios are in a quite narrow range between 0.45-0.71. Similar results have been observed in previous research that considered the graphitization level of carbon produced from difference sources such as waste tyres [20] and plastics [31]. It is difficult to draw any conclusions from these Raman results which is why the TPO was used as a supplementary method to analysis the carbon formed on the Y-zeolite at different temperatures. The TPO quite clearly shows there is a change in the carbon formed as you go to higher temperatures.

Figure 7 shows the TEM micrographs of used Y-zeolite at 400, 500, 600, 700 and 800 °C. Coke was detected in each of the reacted Y-zeolite samples at different temperatures, which is consistent with the TPO results in Figure 4. Amorphous carbon is more obvious in the used Y-zeolite reacted at temperature at 400 and 500 °C and both graphitic and amorphous carbon are observed at relative higher temperatures at 600, 700 and 800 °C. The result could be supported by previous researcher, Lee et al. [35] successfully synthesised a LaY-zeolite templated carbon prepared at high temperature. It has a similar graphitic structure as 3D graphene-like sp^2 hybridized bonds. Amorphous are observed in all of the used Y-zeolite samples, which is consistent with the TPO and Raman results in Figure 4 and Figure 6, respectively. The TPO results in Figure 4 show the coke formed on all of the used Y-zeolite samples oxidise between 350 °C and 700 °C, which indicates that the formed coke on the Y-zeolite surface is a mixture of amorphous and graphitic carbon.

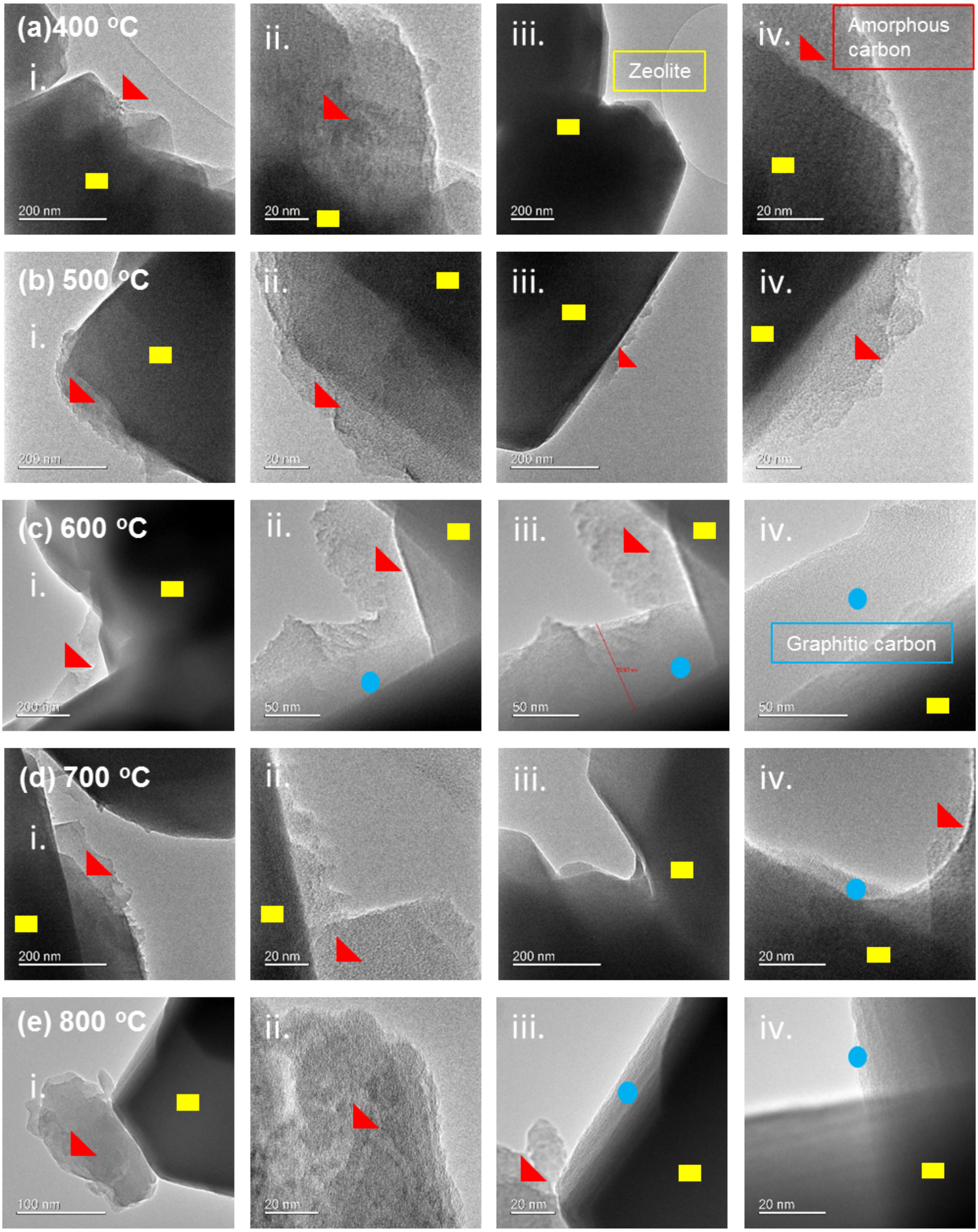
(a)400 °C
i.
200 nm
ii.
20 nm
iii.
Zeolite
200 nm
iv.
Amorphous carbon
20 nm
(b) 500 °C
i.
200 nm
ii.
20 nm
iii.
200 nm
iv.
20 nm
(c) 600 °C
i.
200 nm
ii.
50 nm
iii.
50 nm
iv.
Graphitic carbon
50 nm
(d) 700 °C
i.
200 nm
ii.
20 nm
iii.
200 nm
iv.
20 nm
(e) 800 °C
i.
100 nm
ii.
20 nm
iii.
20 nm
iv.
20 nm

(f)

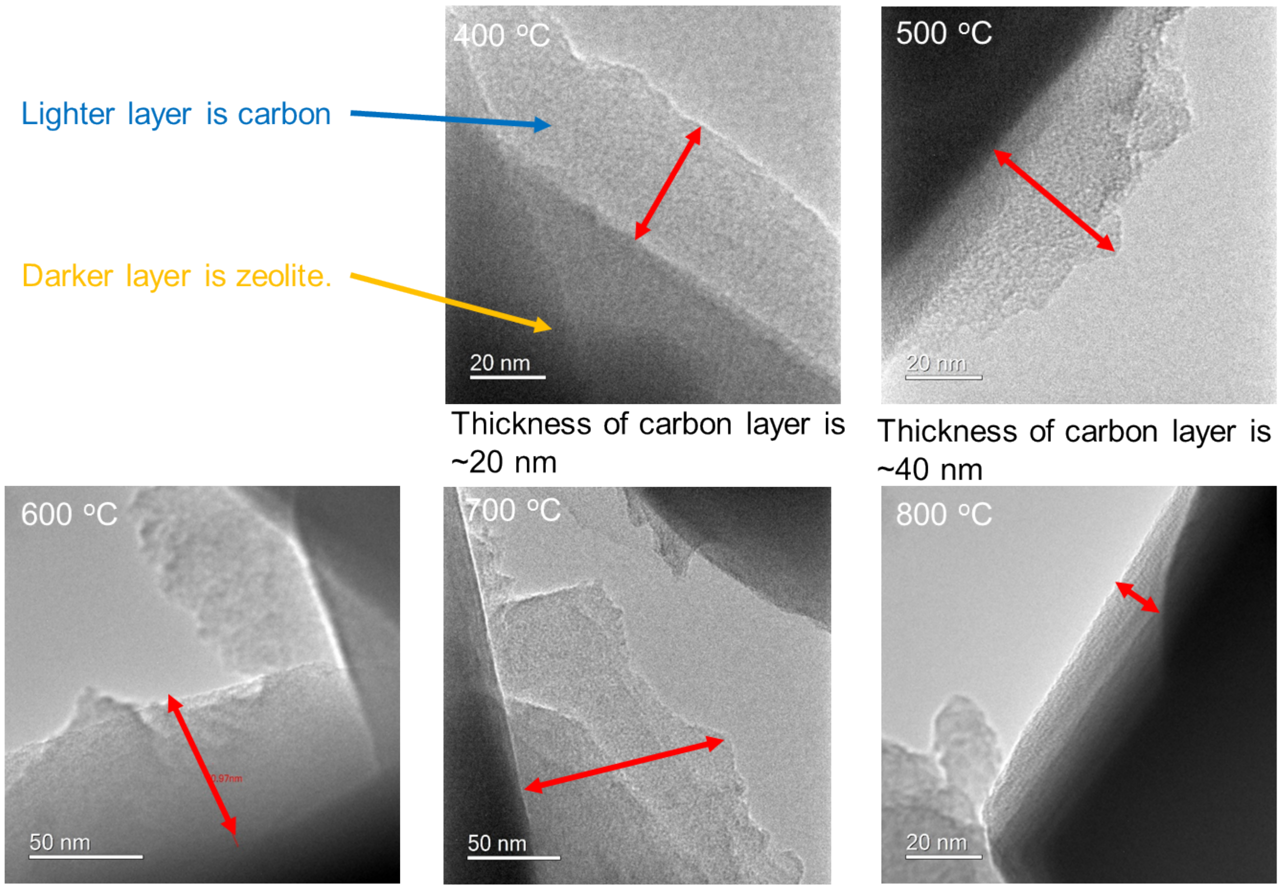

Thickness of carbon layer is ~20 nm

Thickness of carbon layer is ~40 nm

Thickness of carbon layer is ~70 nm

Thickness of carbon layer is ~100 nm

Thickness of carbon layer is ~20 nm

(g)

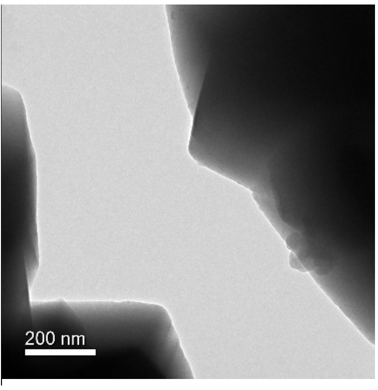

Figure 7 TEM micrographs of reacted Y-zeolite at 400, 500, 600, 700 and 800 °C. (a)-(e) carbon formed at different temperatures on Y-zeolite surface; (f) Estimation of carbon thickness on the Y-zeolite surface; (g) TEM micrograph of fresh Y-zeolite.

The Raman results in Figure 6(a) further supports this as all spectra of the coke formed on the Y-zeolite catalyst surface at different temperatures contain two peaks, one attributable to amorphous carbon the other graphitic. The thicknesses of the carbon layers on Y-zeolite catalyst surface formed at different temperatures are between 20-100 nm, as illustrated in Figure 7(f).

All of the characterisation results indicate that temperature has a strong effect on the nature of the carbon formed, especially at temperature above 600 °C. This finding is consistant with previous reports [21,36]. Acomb et al. [36] investigated the temperature effect on the production of carbon nanotubes from plastics by pyrolysis-catalysis. Previous work conducted by the authors observed that the temperature plays an important role to promote more production of highly graphitized carbon nanotubes. Zhang et al. [21] investigated the highly graphitic filamentous carbon with higher production at a higher temperature of 900 °C compared with 700 °C in the pyrolysis-catalysis of waste plastics.

3.3 Influence of sample-to-catalyst ratio on coke formation

The influence of sample-to-catalyst ratios at 1:1, 2:1, 3:1, 4:1 and 5:1 on coke formation during the volatilization/decomposition of heavy oil has been investigated at 500 °C. The amount of Y-zeolite catalyst was kept constant at 0.5 g for all of the experiments. The used Y-zeolite samples were analysed by using TPO with the results presented in Figure 8 (a). The results show in Figure 8 inset reveal that the increase of sample-to-catalyst ratio increases the quantity of formed coke, as expected, since the amount of carbon precursor increases.

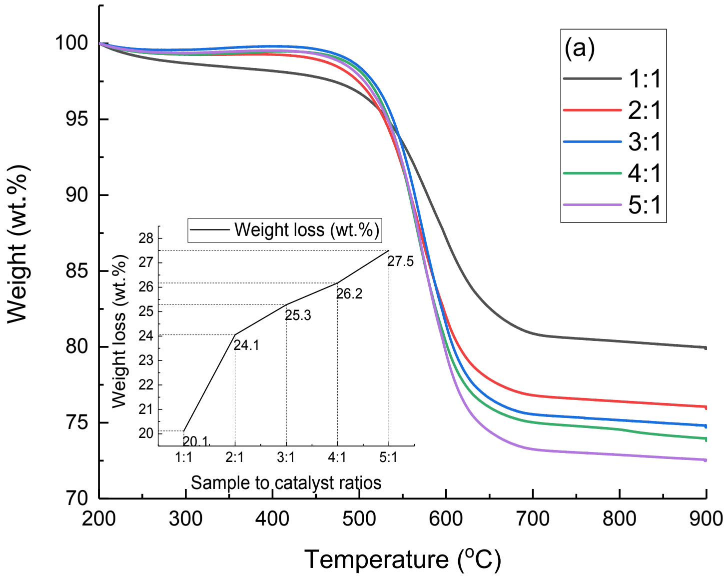

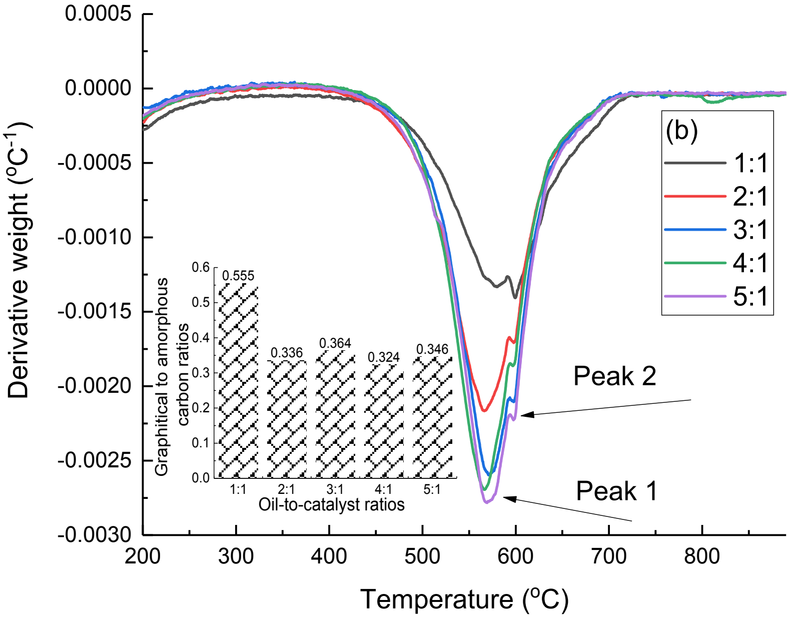

Figure 8 (a)TPO, inset figure is the derived carbon production based on TPO weight loss and (b) DTG results of carbon produced from oil at 500 °C in the presence of Y-zeolite with a sample-to-catalyst ratio of 1:1, 2:1, 3:1, 4:1 and 5:1;(b)Inset, graphitic/amorphous carbon ratios produced at oil-to-catalyst ratio at different oil-to-catalyst ratios.

Figure 8(b) presents the DTG-TPO results of the carbon formed at different sample-to-catalyst ratios. They are all similar with two overlapping oxidation peaks at around 560 (peak 1) and 600 °C (peak 2), respectively. The results indicate the degree of graphitization of the coke formed is not related to the sample-to-catalyst ratio. These results are further confirmed by the Raman analysis, as shown in Figure 9. All the coke samples formed at 500 °C with different sample-to-catalyst ratios have a D-band at 1375 cm^{-1} and G-band at 1590 cm^{-1} as shown in Figure 9 (a). The degree of graphitization of the coke formed at different sample-to-catalyst ratios are similar, with I_D/I_G ratios between 0.505 and 0.817 as shown in Figure 9 (b). The results are supported by other researchers [36]. Acomb et al. [36] found that the increment of feedstock will increase the production of carbon production, especially of highly graphitizated carbon nanotubes. Figure 8 (a)TPO, inset figure is the derived carbon production based on TPO weight loss and (b) DTG results of carbon produced from oil at 500 °C in the presence of Y-zeolite with a sample-to-catalyst ratio of 1:1, 2:1, 3:1, 4:1 and 5:1;(b)Inset, graphitic/amorphous carbon ratios produced at oil-to-catalyst ratio at different oil-to-catalyst ratios. Figure 8 (b) inset shows the quantitative ratios of graphitic/amorphous carbon are in different trend, where the 1:1 ratio gave the highest ratio at 0.555. The graphitic/amorphous ratios of carbon produced at other oil-to-catalyst ratios (2:1, 3:1, 4:1 and 5:1) are similar ~ 0.34 ± 0.023. This could relates to the deactivation of the catalyst occurs at oil-to-catalyst ratio at 1:1, the further increase amount of the oil will not lead to graphitic carbon growth but the amorphous carbon .

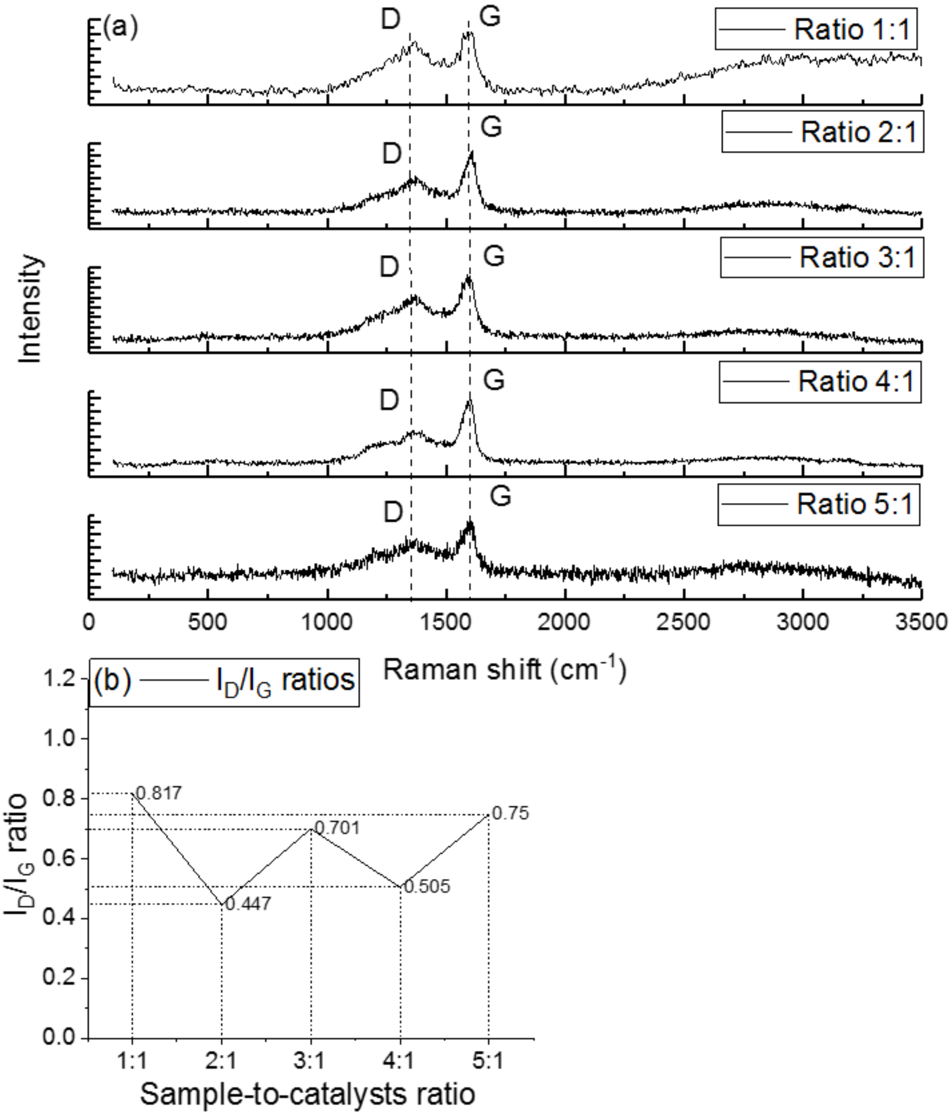

Figure 9 (a)Raman results of carbon produced from oil at 500 °C in the presence of Y- zeolite with sample-to-catalyst ratios of 1:1, 2:1, 3:1, 4:1 and 5:1; (b) I_D/I_G ratios.

4 Conclusion

Coke was found in all of the used Y-zeolite samples following volatilization/decomposition of heavy oil in a tubular reactor, regardless of reaction temperature and sample-to-catalyst ratios. However, the volatilization/decomposition temperature plays an important role on the formation of coke to deactivate the catalyst in terms of the graphitization level, but not the quantity of the carbon formed on Y-zeolite catalyst. Although the volatilization/decomposition temperature increased from 400 to 800 ^{o}C, the quantity of coke production is in a small range of 23-24% per gram of heavy oil sample. The higher temperatures of 700 and 800 ^{o}C promote more graphitic carbon production, with graphitic-to-amorphous ratios of 0.89 and 0.82, respectively. Lower temperatures, 400, 500 and 600 ^{o}C, hinder the graphitic carbon formation, which is approximately half of the graphitic carbon produced at temperatures above 600 ^{o}C. The results have been confirmed by TPO and TEM analysis. But it is difficult to analysis coke based on Raman spectra whereas TPO is an ideal technique to reveal more information about the nature of the carbon grown on Y-zeolite at different temperature in heavy oil thermal cracking process. The sample-to-catalyst ratio plays a significant role in the quantity of coke formed, rather than on the graphitic-to-amorphous ratio as the carbon source is increased but not the formation temperature. Higher sample-to-catalyst ratios form higher amounts of coke on Y-zeolite catalyst, as confirmed by TPO and Raman spectroscopy.

Acknowledgements

This work is financially supported by Qatar National Research Fund (QNRF) from National Priority Research Program (NPRP9-313-2-135).

References:

[1] R. Sahu, B.J. Song, J.S. Im, Y.-P. Jeon and C.W. Lee, A review of recent advances in catalytic hydrocracking of heavy residues, *Journal of Industrial and Engineering Chemistry*, 27, (2015) 12, https://doi.org/10.1016/j.jiec.2015.01.011.

[2] EIA, in, Energy Information Administration Office of Integrated Analysis and Forecasting U.S. Department of Energy, 2003.

[3] H. Shen, Z. Ding and R. Li, Thermal conversion - an efficient way for heavy residue processing, *Proc. 15th World Petroleum Congress*, 2, (1998) 907.

[4] J.G. Speight, *The desulfurization of heavy oils and residua*, CRC Press, 1999, 294.

[5] K. Akubo, M.A. Nahil and P.T. Williams, Aromatic fuel oils produced from the pyrolysis-catalysis of polyethylene plastic with metal-impregnated zeolite catalysts, *Journal of the Energy Institute*, 92, (2019) 195, https://doi.org/10.1016/j.joei.2017.10.009.

[6] B.C. Gates, Catalytic chemistry, (1991).

[7] A.T. Sipra, N. Gao and H. Sarwar, Municipal solid waste (MSW) pyrolysis for bio-fuel production: A review of effects of MSW components and catalysts, *Fuel Processing Technology*, 175, (2018) 131, https://doi.org/10.1016/j.fuproc.2018.02.012.

[8] Y.S. Choi, Y. Elkasabi, P.C. Tarves, C.A. Mullen and A.A. Boateng, Catalytic cracking of fast and tail gas reactive pyrolysis bio-oils over HZSM-5, *Fuel Processing Technology*, 161, (2017) 132, https://doi.org/10.1016/j.fuproc.2017.03.019.

[9] B. Wang and G. Manos, A novel thermogravimetric method for coke precursor characterisation, *Journal of Catalysis*, 250, (2007) 121, https://doi.org/10.1016/j.jcat.2007.05.018.

[10] S. Chen and G. Manos, In situ thermogravimetric study of coke formation during catalytic cracking of normal hexane and 1-hexene over ultrastable Y zeolite, *Journal of Catalysis*, 226, (2004) 343, https://doi.org/10.1016/j.jcat.2004.06.004.

[11] Á. Ibarra, A. Veloso, J. Bilbao, J.M. Arandes and P. Castaño, Dual coke deactivation pathways during the catalytic cracking of raw bio-oil and vacuum gasoil in FCC conditions, *Applied Catalysis B: Environmental*, 182, (2016) 336, https://doi.org/10.1016/j.apcatb.2015.09.044.

[12] Y. Li, C. Zhang, Y. Liu, S. Tang, G. Chen, R. Zhang and X. Tang, Coke formation on the surface of Ni/HZSM-5 and Ni-Cu/HZSM-5 catalysts during bio-oil hydrodeoxygenation, *Fuel*, 189, (2017) 23, https://doi.org/10.1016/j.fuel.2016.10.047.

[13] M. Materazzi, F. Grimaldi, P.U. Foscolo, P. Cozens, R. Taylor and C. Chapman, Analysis of syngas methanation for bio-SNG production from wastes: kinetic model development and pilot scale validation, *Fuel Processing Technology*, 167, (2017) 292, https://doi.org/10.1016/j.fuproc.2017.07.009

[14] C.H. Bartholomew, Mechanisms of catalyst deactivation, *Applied Catalysis A: General*, 212, (2001) 17, https://doi.org/10.1016/S0926-860X(00)00843-7.

[15] M. Guisnet and P. Magnoux, Organic chemistry of coke formation, *Applied Catalysis A: General*, 212, (2001) 83, https://doi.org/10.1016/S0926-860X(00)00845-0.

[16] H.S. Cerqueira, G. Caeiro, L. Costa and F. Ramôa Ribeiro, Deactivation of FCC catalysts, *Journal of Molecular Catalysis A: Chemical*, 292, (2008) 1, https://doi.org/10.1016/j.molcata.2008.06.014.

[17] M.S. Rana, J. Ancheyta, S.K. Sahoo and P. Rayo, Carbon and metal deposition during the hydroprocessing of Maya crude oil, *Catalysis Today*, 220, (2014) 97, https://doi.org/10.1016/j.cattod.2013.09.030.

[18] A. Demirbas, H. Alidrisi and M.A. Balubaid, API Gravity, Sulfur Content, and Desulfurization of Crude Oil, *Petroleum Science and Technology*, 33, (2015) 93, https://doi.org/10.1080/10916466.2014.950383.

[19] C. Wu and P.T. Williams, Investigation of coke formation on Ni-Mg-Al catalyst for hydrogen production from the catalytic steam pyrolysis-gasification of polypropylene, *Applied Catalysis B: Environmental*, 96, (2010) 198, http://dx.doi.org/10.1016/j.apcatb.2010.02.022.

[20] Y. Zhang and P.T. Williams, Carbon nanotubes and hydrogen production from the pyrolysis catalysis or catalytic-steam reforming of waste tyres, *Journal of Analytical and Applied Pyrolysis*, 122, (2016) 490, https://doi.org/10.1016/j.jaap.2016.10.015.

[21] Y. Zhang, M.A. Nahil, C. Wu and P.T. Williams, Pyrolysis–catalysis of waste plastic using a nickel–stainless-steel mesh catalyst for high-value carbon products, *Environmental technology*, 38, (2017) 1, https://doi.org/10.1080/09593330.2017.1281351.

[22] W. Fang, C. Pirez, M. Capron, S. Paul, T. Raja, P.L. Dhepe, F. Dumeignil and L. Jalowiecki-Duhamel, Ce-Ni mixed oxide as efficient catalyst for H2 production and nanofibrous carbon material from ethanol in the presence of water, *RSC Advances*, 2, (2012) 9626, https://doi.org/10.1039/c2ra21701e.

[23] M.S. Dresselhaus, G. Dresselhaus, A. Jorio, A.G. Souza Filho and R. Saito, Raman spectroscopy on isolated single wall carbon nanotubes, *Carbon*, 40, (2002) 2043, http://dx.doi.org/10.1016/S0008-6223(02)00066-0.

[24] A. Carrero, J.A. Calles and A.J. Vizcaíno, Effect of Mg and Ca addition on coke deposition over Cu–Ni/SiO2 catalysts for ethanol steam reforming, *Chemical Engineering Journal*, 163, (2010) 395, http://dx.doi.org/10.1016/j.cej.2010.07.029.

[25] R.A. DiLeo, B.J. Landi and R.P. Raffaelle, Purity assessment of multiwalled carbon nanotubes by Raman spectroscopy, *Journal of Applied Physics*, 101, (2007) 064307, doi:http://dx.doi.org/10.1063/1.2712152.

[26] A.C. Ferrari and J. Robertson, Raman spectroscopy of amorphous, nanostructured, diamond–like carbon, and nanodiamond, *Philosophical Transactions of the Royal Society of London A: Mathematical, Physical and Engineering Sciences*, 362, (2004) 2477, https://doi.org/10.1098/rsta.2004.1452.

[27] M.W. Smith, I. Dallmeyer, T.J. Johnson, C.S. Brauer, J.-S. McEwen, J.F. Espinal and M. Garcia-Perez, Structural analysis of char by Raman spectroscopy: Improving band assignments through computational calculations from first principles, *Carbon*, 100, (2016) 678, https://doi.org/10.1016/j.carbon.2016.01.031.

[28] A.C. Ferrari and J. Robertson, Interpretation of Raman spectra of disordered and amorphous carbon, *Physical review B*, 61, (2000) 14095, https://doi.org/10.1103/PhysRevB.61.14095.

[29] Z. Li, K. Xie and R.C. Slade, Studies of the interaction between CuCl and HY zeolite for preparing heterogeneous CuI catalyst, *Applied Catalysis A: General*, 209, (2001) 107, https://doi.org/10.1016/S0926-860X(00)00745-6.

[30] N.A.S. Ramli and N.A.S. Amin, Fe/HY zeolite as an effective catalyst for levulinic acid production from glucose: characterization and catalytic performance, *Applied Catalysis B: Environmental*, 163, (2015) 487, https://doi.org/10.1016/j.apcatb.2014.08.031.

[31] Y. Zhang, C. Wu, M.A. Nahil and P. Williams, High-value resource recovery products from waste tyres, *Proceedings of the Institution of Civil Engineers–Waste and Resource Management*, 169, (2016) 137, https://doi.org/10.1680/jwarm.16.00001.

[32] J. Robertson, Diamond-like amorphous carbon, *Materials Science and Engineering: R: Reports*, 37, (2002) 129, https://doi.org/10.1016/S0927-796X(02)00005-0.

[33] P.R. Somani and M. Umeno, Importance of transmission electron microscopy for carbon nanomaterials research, *Modern Research and Educational Topics in Microscopy*, 3, (2007) 634.

[34] H. Heise, R. Kuckuk, A. Ojha, A. Srivastava, V. Srivastava and B. Asthana, Characterisation of carbonaceous materials using Raman spectroscopy: a comparison of carbon nanotube filters, single- and multi- walled nanotubes, graphitised porous carbon and graphite, *Journal of Raman Spectroscopy*, 40, (2009) 344, https://doi.org/10.1002/jrs.2120.

[35] H. Lee, K. Kim, S.-H. Kang, Y. Kwon, J. Hun Kim, Y.-K. Kwon, R. Ryoo and J. Young Park, Extremely high electrical conductance of microporous 3D graphene-like zeolite-templated carbon framework, *Scientific reports*, 7, (2017), https://doi.org/10.1038/s41598-017-11602-5.

[36] J.C. Acomb, C. Wu and P.T. Williams, Effect of growth temperature and feedstock:catalyst ratio on the production of carbon nanotubes and hydrogen from the pyrolysis of waste plastics, *Journal of Analytical and Applied Pyrolysis*, 113, (2015) 231, http://dx.doi.org/10.1016/j.jaap.2015.01.012.